

Global Biogeochemical Cycles®

REVIEW ARTICLE

10.1029/2024GB008254

Special Collection:

The Elements Collection

Key Points:

- We compile existing rhenium (Re) concentration data and flux estimates in Earth's surface reservoirs
- Although rhenium is one of the rarest elements in the Earth's crust, human activity has enhanced Re mobilization by around 3- to 4-fold
- Rhenium may help track the oxidation of rock-bound organic carbon, track anthropogenic pollution, and reconstruct paleoredox conditions

Supporting Information:

Supporting Information may be found in the online version of this article.

Correspondence to:

L. Ghazi and J. C. Pett-Ridge,
ghazi@oregonstate.edu;
Julie.Pett-Ridge@oregonstate.edu

Citation:

Ghazi, L., Grant, K. E., Chappaz, A., Danish, M., Peucker-Ehrenbrink, B., & Pett-Ridge, J. C. (2024). The global biogeochemical cycle of rhenium. *Global Biogeochemical Cycles*, 38, e2024GB008254. <https://doi.org/10.1029/2024GB008254>

Received 14 JUN 2024

Accepted 11 SEP 2024

Author Contributions:

Conceptualization: L. Ghazi, J. C. Pett-Ridge
Data curation: L. Ghazi, K. E. Grant, A. Chappaz, M. Danish, B. Peucker-Ehrenbrink, J. C. Pett-Ridge
Formal analysis: L. Ghazi, K. E. Grant, A. Chappaz, M. Danish, B. Peucker-Ehrenbrink, J. C. Pett-Ridge
Investigation: K. E. Grant, A. Chappaz, M. Danish, B. Peucker-Ehrenbrink, J. C. Pett-Ridge
Project administration: L. Ghazi
Visualization: L. Ghazi, K. E. Grant, A. Chappaz, M. Danish, J. C. Pett-Ridge
Writing – original draft: L. Ghazi, K. E. Grant, A. Chappaz, M. Danish, B. Peucker-Ehrenbrink, J. C. Pett-Ridge

© 2024. American Geophysical Union. All Rights Reserved.

The Global Biogeochemical Cycle of Rhenium

L. Ghazi¹ , K. E. Grant² , A. Chappaz³ , M. Danish⁴ , B. Peucker-Ehrenbrink⁵ , and J. C. Pett-Ridge^{1,6} 

¹College of Earth, Ocean, and Atmospheric Sciences, Oregon State University, Corvallis, OR, USA, ²Center for Accelerator Mass Spectrometry, Lawrence Livermore National Laboratory, Livermore, CA, USA, ³STARLAB, Department of Earth and Atmospheric Sciences, Central Michigan University, Mount Pleasant, MI, USA, ⁴Dr. Moses Strauss Department of Marine Geosciences, The Leon H. Charney School of Marine Sciences, University of Haifa, Carmel, Israel, ⁵Marine Chemistry and Geochemistry Department, Woods Hole Oceanographic Institution, Woods Hole, MA, USA, ⁶Department of Crop and Soil Sciences, College of Agricultural Sciences, Oregon State University, Corvallis, OR, USA

Abstract This paper is the first comprehensive synthesis of what is currently known about the different natural and anthropogenic fluxes of rhenium (Re) on Earth's surface. We highlight the significant role of anthropogenic mobilization of Re, which is an important consideration in utilizing Re in the context of a biogeochemical tracer or proxy. The largest natural flux of Re derives from chemical weathering and riverine transport to the ocean (dissolved = $62 \times 10^6 \text{ g yr}^{-1}$ and particulate = $5 \times 10^6 \text{ g yr}^{-1}$). This review reports a new global average [Re] of $16 \pm 2 \text{ pmol L}^{-1}$, or $10 \pm 1 \text{ pmol L}^{-1}$ for the inferred pre-anthropogenic concentration without human impact, for rivers draining to the ocean. Human activity via mining (including secondary mobilization), coal combustion, and petroleum combustion mobilize approximately $560 \times 10^6 \text{ g yr}^{-1}$ Re, which is more than any natural flux of Re. There are several poorly constrained fluxes of Re that merit further research, including: submarine groundwater discharge, precipitation (terrestrial and oceanic), magma degassing, and hydrothermal activity. The mechanisms and the main host phases responsible for releasing (sources) or sequestering (sinks) these fluxes remain poorly understood. This study also highlights the use of dissolved [Re] concentrations as a tracer of oxidation of petrogenic organic carbon, and stable Re isotopes as proxies for changes in global redox conditions.

Plain Language Summary This study examines how the rare element rhenium (Re) moves throughout the Earth's surface. The largest natural source of Re is rock weathering, but human activities such as mining, coal combustion, and petroleum combustion have accelerated the natural Re cycle. Understanding the behavior of Re in a variety of Earth surface environments helps us to evaluate fundamental biogeochemical questions about Earth's carbon and oxygen cycles.

1. Introduction

Rhenium (Re) is one of the rarest elements on the Earth's surface, with an average concentration in the upper continental crust estimated to be $200\text{--}400 \text{ pg g}^{-1}$ (Esser & Turekian, 1993; McLennan, 2001; Peucker-Ehrenbrink & Jahn, 2001; Taylor & McLennan, 1985; Wedepohl, 1995) (Table S1 in Supporting Information S1). Walter Noddack, Ida Noddack-Tacke, and Otto Berg are generally considered to have discovered the last naturally occurring element using x-ray emission lines (Noddack et al., 1925; Noddack & Noddack, 1927). The element, which they named in honor of Europe's Rhine River, was isolated from the minerals columbite, gadolinite and molybdenite (Noddack et al., 1925). However, it has also been suggested that Re was first discovered by Masataka Ogawa in 1908 when he isolated what later became known as Re from thorianite (ThO_2) and identified the unknown material using x-ray spectra (Hisamatsu et al., 2022). Upon this discovery, Ogawa identified this element as the missing element 43 (now known as technetium) and gave it the name nipponium (Ogawa, 1908a, 1908b). Contemporary examinations of the chemical and physical characteristics of nipponium revealed the similarity between nipponium and Re, but due to lack of access to sophisticated scientific infrastructure and resources for follow-up studies, the tentative discovery of nipponium as the element Re is considered later historically. Subsequently, studies and attempts at mass production confirmed that few Re dominated minerals exist. Rheniite (ReS_2) is the only mineral known to contain Re as its primary metal constituent (Znamensky et al., 2005); however, this mineral typically does not appear in sufficient quantities to facilitate economic extraction; thus, Re metal is mainly extracted from molybdenite and copper sulfide minerals (Naumov, 2007). Porphyry copper mines in Chile account for about 55% of global Re production (John et al., 2017). There is little

Writing – review & editing: L. Ghazi, K. E. Grant, A. Chappaz, M. Danish, B. Peucker-Ehrenbrink, J. C. Pett-Ridge

demand for pure Re objects, but Re is highly desirable as an addition to alloys because it has an extremely high melting point (3185°C) and it enhances metal strength and ductility (Anderson et al., 2013). Rhenium alloys are used in nuclear reactors, semiconductors, electronics, filaments, and aerospace applications (John et al., 2017; Kablov et al., 2006; Naumov, 2007). Rhenium also plays an important role in the chemicals industry as a highly selective catalyst in hydrogenation reactions of fine chemicals (Broadbent et al., 1959; John et al., 2017).

Table 1 highlights some of the key chemical characteristics of Re. Rhenium oxidation states range between -1 and $+7$ (Maun & Davidson, 1950), but $+4$ and $+7$ are the most common at the Earth's surface (John et al., 2017; Yamashita et al., 2007). There are two naturally occurring isotopes of Re: ^{187}Re (62.6%) and ^{185}Re (37.4%) (Gramlich et al., 1973; White & Cameron, 1948). The ^{185}Re isotope is stable; however, the ^{187}Re isotope is metastable (Naldrett & Libby, 1948) and β -decays to ^{187}Os with a half-life of 4.16×10^{10} years (Herr et al., 1954; Selby et al., 2007; Shen et al., 1996; Smoliar et al., 1996). This radiogenic production of ^{187}Os forms the basis for using Re-Os isotope systematics as a geochronometer (Geiss et al., 1958; Yin et al., 1993). The ^{187}Re – ^{187}Os geochronometer has been applied to the determination of depositional ages of sulfide-rich and organic-rich sediment, coal, timescales of petroleum generation, origins and ages of extraterrestrial objects, and periods of changes in the Earth's carbon cycle (Allègre & Luck, 1980; Anbar et al., 2007; Cohen et al., 1999; Esser & Turekian, 1993; Herr et al., 1962; Hintenberger et al., 1954; Kendall et al., 2004; Luck et al., 1980; Naldrett & Libby, 1948; Ravizza & Turekian, 1989; Riley, 1967; Riley & Delong, 1970; Rooney et al., 2012; Selby & Creaser, 2003, 2005; Selby et al., 2007; Shirey & Walker, 1998; Suttle & Libby, 1954; Tripathy et al., 2015; Turekian & Luck, 1984). Although the specific use of the Re-Os as a geochronometer and in high-temperature geochemistry is beyond the scope of this paper, we note that these fields have contributed to the advancement of analytical methods used to precisely measure Re and its isotopes.

Under oxic conditions, dissolved Re is thought to be present as the soluble oxyanion perrhenate ($\text{Re(VII)}\text{O}_4^-$), which is stable across a wide range of pH (0–14) and Eh (0.3–1 V) conditions (Brookins, 1986; Nikolaychuk, 2022). Dissolved Re is thought to behave mostly conservatively in oxygenated soil porewaters, groundwater, rivers, and ocean environments (Anbar et al., 1992; Colodner et al., 1993; Hodge et al., 1996). In estuaries, Re behavior is not well understood and exhibits both conservative and non-conservative mixing patterns (Anbar et al., 1992; Brookins, 1986; Colodner et al., 1993; Koide et al., 1986; Sheen et al., 2018). In marine sediments, dissolved Re concentrations decrease significantly across oxic-anoxic boundaries (e.g., Colodner et al., 1993; Helz, 2022; Morford et al., 2007). Such gradients lead to Re-enriched sediments in reducing environments, with Re concentrations 100 to 1000-fold above average crustal values (e.g., Bennett & Canfield, 2020; Colodner et al., 1993; Ravizza et al., 1991). This contrasting geochemical behavior between oxic and anoxic conditions has led to the use of Re as a paleoredox proxy for determining the redox conditions that were prevailing at the time of deposition in ancient sedimentary systems. Additionally, geoscientists who study the behavior of radioactive materials use Re as an analog of technetium (Tc), a primarily artificial radioactive element, because of their similar speciation and redox behavior (Kim et al., 2004; Wakoff & Nagy, 2004). Given the significant positive correlations between Re and organic matter enrichments in sedimentary settings (Cohen et al., 1999; Colodner et al., 1993; Jaffe et al., 2002; Ravizza et al., 1991), Re has been used as a proxy to trace the CO_2 release from oxidation of petrogenic organic carbon (OC_{petro}) in those sedimentary rocks when they are exposed at Earth's surface (Hilton et al., 2014; Horan et al., 2019). Recently, the potential use of stable Re isotopes as a paleoredox proxy and terrestrial weathering proxy has been proposed (Dellinger et al., 2020, 2021; Dickson et al., 2020; Miller et al., 2009, 2015).

^{187}Re undergoes β^- decay to become ^{187}Os

Half life of radioactive decay^{a,b,c,d} 4.16×10^{10} years

δ -notation of stable Re isotopes

$\delta^{187}\text{Re} (\%) = [({}^{187}\text{Re/}{}^{185}\text{Re}_{\text{sample}})/({}^{187}\text{Re/}{}^{185}\text{Re}_{\text{NIST3143}}) - 1] * 1,000$

Physical properties^e

Phase at STP Solid (silverish-gray)

Melting point 3459 K (3,186°C, 5,767°F)

Boiling point 5903 K (5,630°C, 10,170°F)

Crystalline structure Hexagonal Close Packed (HCP)

Specific gravity 20.5 at 20°C (68°F)

^aHerr et al. (1954). ^bShen et al. (1996). ^cSmoliar et al. (1996). ^dSelby et al. (2007). ^eBrenan (2018).

This review provides a new synthesis of the reactions and fluxes of Re and its isotopes in Earth's near-surface environment from both natural processes and anthropogenic activities, including the mobilization of Re from rock weathering, mining, and fossil fuel combustion, the transport of Re in dissolved and

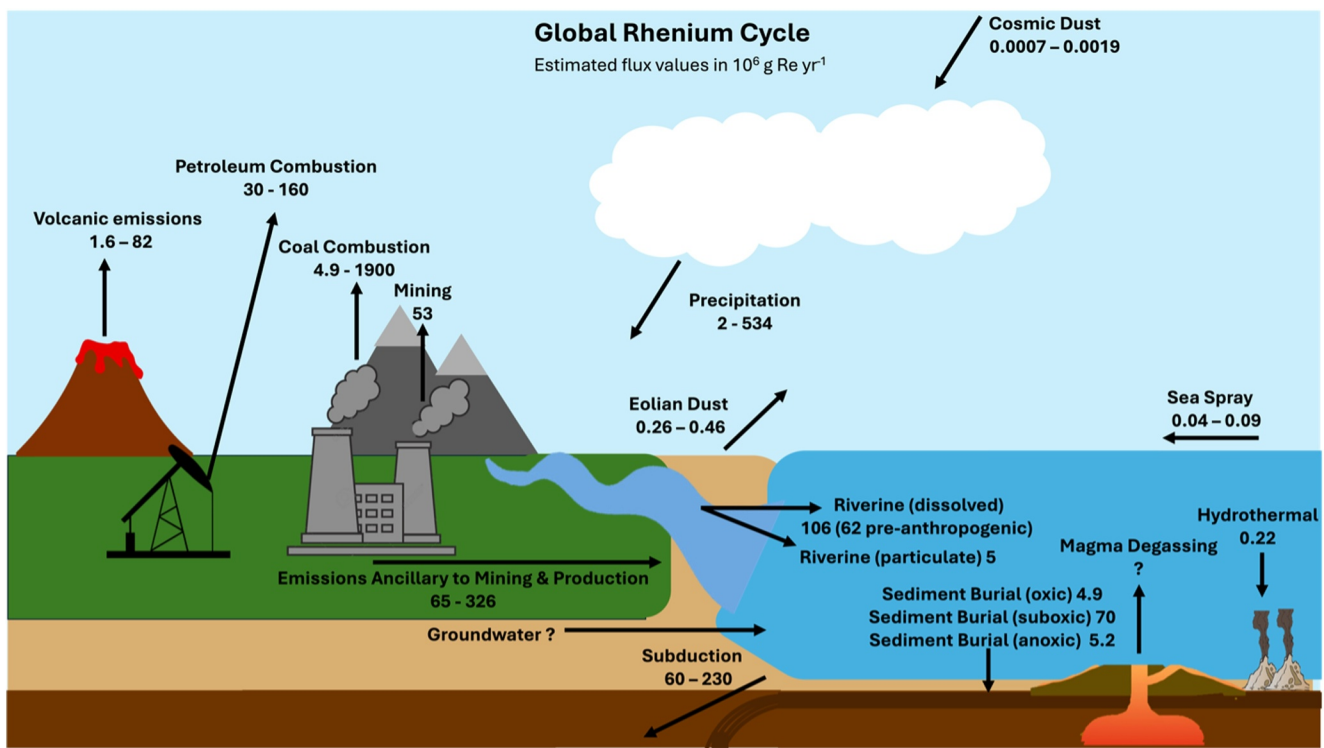


Figure 1. The global biogeochemical cycle of rhenium (Re) showing annual fluxes in 10^6 g yr^{-1} . Estimates are presented throughout the text and in Supporting Information S1.

particulate form in rivers, and inputs of Re to the atmosphere (Figure 1 and Table S2 in Supporting Information S1). We synthesize what is known about Re inputs to the oceans and Re behavior in estuaries, and also biogeochemical controls on Re burial in ocean sediments. This study also collates what is known about Re in terrestrial and marine biota. Additionally, we include summaries of the primary applications of Re as a tracer of Earth's surface biogeochemical processes in modern and over geologic timescales, including its use as a paleoredox tracer, its use in quantifying geologic respiration, the emerging use of Re isotopes to trace rock weathering processes, and the use of Re as a tracer of anthropogenic pollution. Throughout this synthesis, we highlight the important influence of anthropogenic activities on the modern Re cycle and also the areas of greatest uncertainty in Re cycling.

2. The Modern Biogeochemical Cycle

2.1. Terrestrial Environment

2.1.1. Rock Weathering

Geochemically, Re is classified as siderophile, chalcophile, and organophilic (Rooney et al., 2012). Among rock types, black shales with organic carbon content $>1\%$ tend to have the highest concentrations of Re (median value $23,300 \text{ pg g}^{-1}$, 1st and 3rd quartiles $14,600\text{--}51,700 \text{ pg g}^{-1}$, $n = 2234$) (Figure 2 and Table S1 in Supporting Information S1). Fine-grained sedimentary rocks such as gray shales ($<1\%$ organic carbon) have the next highest concentration of Re (median value $3,200 \text{ pg g}^{-1}$, 1st and 3rd quartiles $1,700\text{--}6,000 \text{ pg g}^{-1}$, $n = 754$). Global lithologic mapping indicates that black shales cover 0.3% of Earth's surface rocks, while fine-grained sedimentary rocks cover 35% (Hartmann & Moosdorf, 2012). Therefore, while black shales are locally very important as sources of Re weathering, more common fine-grained sedimentary rocks are likely the dominant source of Re released by weathering globally (Zondervan et al., 2023). Weathered black shales tend to have concentration ranges similar to gray shales (median value $2,000 \text{ pg g}^{-1}$, 1st and 3rd quartiles $1,300\text{--}33,200 \text{ pg g}^{-1}$, $n = 5$ weathering profiles). Other sedimentary rocks have much lower Re concentrations (median value 190 pg g^{-1} , 1st and 3rd quartiles $40\text{--}680 \text{ pg g}^{-1}$, $n = 26$), similar to Re concentrations in most igneous and metamorphic rocks (Figure 2 and Table S1 in Supporting Information S1). Compared to other igneous and metamorphic rocks, acid

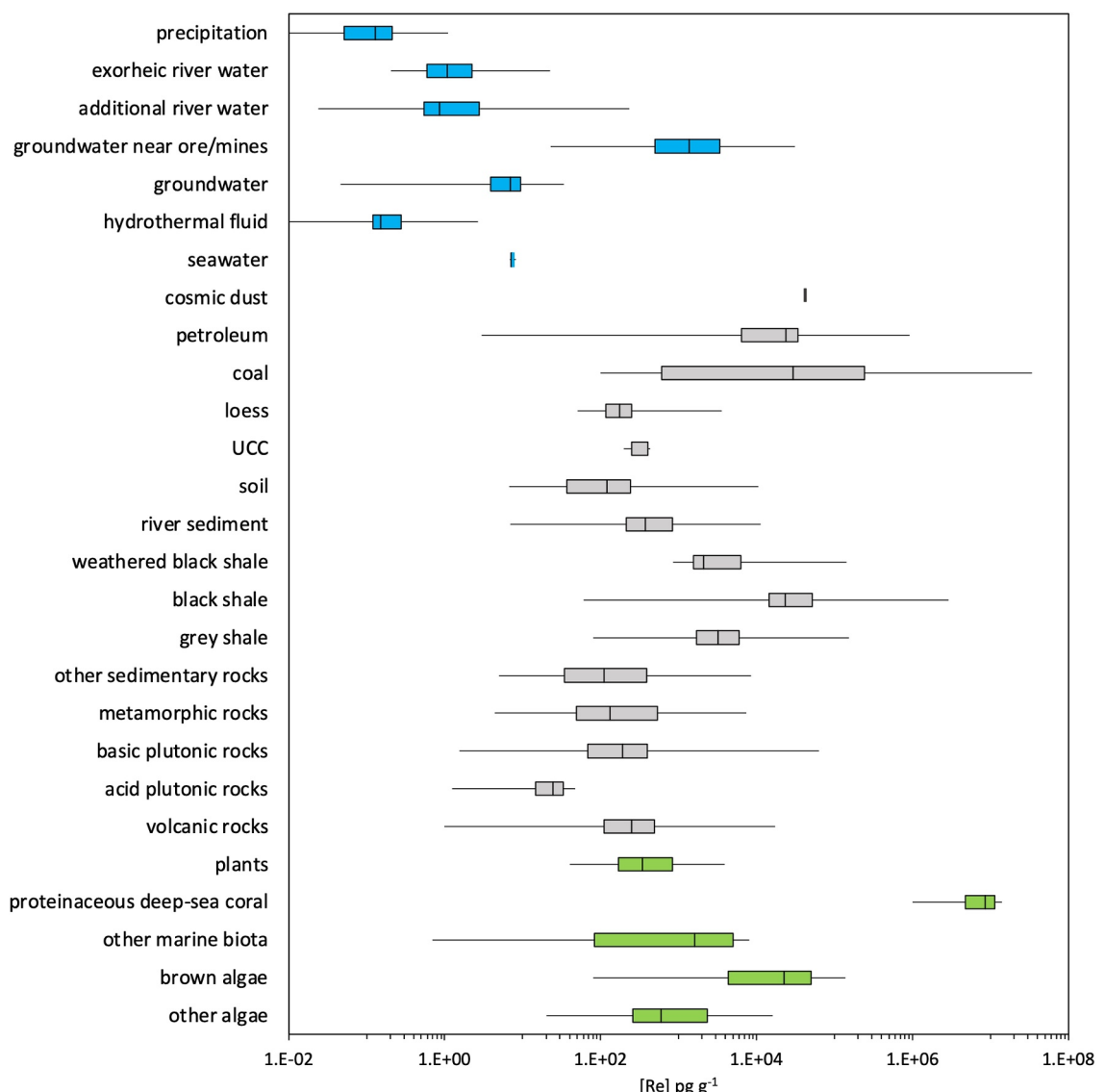


Figure 2. Comparison of reported Re concentration values, including aqueous (blue), biotic (green) and inorganic solids (gray). The vertical line inside the bar represents the median value, the left and right boundaries of each bar represent the 1st and 3rd quartiles, and the whiskers represent the maximum and minimum values. UCC is the upper continental crust. This figure presents Re concentration in mass units. Throughout the manuscript, solid phase geochemistry is presented in mass units and dissolved phase geochemistry data is presented in molar units based on discipline conventions. The full data compilation and references are listed in the Supplementary data tables. References for these data are also included in the supplementary tables.

plutonic rocks have approximately 10-fold lower Re concentrations. Relatively few studies have examined the partitioning of Re during magmatic processes; while magnetite, garnet, and pyrite have been identified as host phases of Re, Re is thought to be moderately incompatible with the primary silicate phases during mantle melting (e.g., Lassiter, 2003; Righter et al., 1998; Wang et al., 2024).

Chemical weathering mobilizes Re, and there are multiple specific mechanisms that may be responsible for Re release, including sulfide oxidation, oxidation of OC_{petro} , and dissolution of silicate minerals. Partitioning of source phases for dissolved Re can be calculated using typical Na/Re ratios of silicate minerals and S/Re ratios sulfide minerals, respectively, followed with an assumption that the remaining fraction is associated with OC_{petro} (Dellinger et al., 2023; Hilton et al., 2021; Horan et al., 2019; Rout & Tripathy, 2024; Zondervan et al., 2023). In the tropical Mahanadi River basin (India), oxidation of OC_{petro} is the primary source of Re, accounting for $85 \pm 10\%$ of the total contribution. Other sources such as silicates and sulfides were found to account for only $13 \pm 8\%$ and $2 \pm 2\%$ of the total contribution, respectively (Rout & Tripathy, 2024). The same approach for rivers in the

Mackenzie River basin, the Rio Madre de Dios in the Andes, and small alpine streams in Switzerland and Colorado similarly found that >75% of Re was derived from oxidation of OC_{petro} (Dellinger et al., 2023; Hilton et al., 2021; Horan et al., 2019). Rhenium apportionment among different phases within rocks has also been investigated using sequential extraction approaches, designed to distinguish, for example, Re associated with organic and sulfide phases (presumably extracted with aqua regia) from Re associated with silicate and other more resistant phases (extracted with hydrofluoric acid). For both suspended river sediments from the Mackenzie River basin, and for a weathered black shale profile in China, the majority of the Re was extracted using aqua regia (Dellinger et al., 2021; Zhang et al., 2024). This approach is somewhat limited, however, by the non-specificity of the extractants.

Rhenium weathering has also been studied by examining patterns of Re loss with depth in soil and rock weathering profiles. Overall, these studies show that Re is highly mobile. For example, black shale weathering profiles from Kentucky and the Nepal Himalaya show 92%–97% Re loss during weathering (Jaffe et al., 2002; Pierson-Wickmann et al., 2002), black shale weathering profiles from Quebec show 25%–64% Re loss (Peucker-Ehrenbrink & Hannigan, 2000), and a deep gray shale weathering profile from Pennsylvania shows ~90% Re loss (Ogrič et al., 2023). Soil weathering profiles also show large losses of Re relative to underlying bedrock (Figure 2 and Table S1 in Supporting Information S1).

The kinetics of Re release are not well known relative to the kinetics of sulfide oxidation, dissolution of primary minerals, and oxidation of OC_{petro}. However, the relative loss patterns in weathering profiles can indicate Re host phases and their relative weathering rates. In particular, the potential use of Re as a tracer of georespiration (Section 4.2) motivates the question of whether Re is hosted in OC_{petro}, and the question of relative weathering rates of OC_{petro} oxidation. Weathering profiles show that loss of S driven by oxidation of sulfide minerals often occurs at greater depth and thus more quickly than the loss of OC_{petro} via oxidation (Gu et al., 2020; Jaffe et al., 2002; Petsch et al., 2000; Wan et al., 2019; Zhang et al., 2024). Two black shale weathering profiles similarly show that S is lost more abruptly and/or at greater depth than Re (Hilton et al., 2021; Zhang et al., 2024). The available data is still quite limited, however, and we note that a separate study of a gray shale weathering profile in a slowly denuding landscape had indistinguishable zones of OC_{petro} depletion, pyrite depletion, and Re depletion (Ogrič et al., 2023). One additional approach to identifying the relative depth and rate of Re and S weathering is to compare the slope of concentration-discharge relationships for dissolved Re and S in rivers. In the Eel and Umpqua rivers in the Pacific Northwest, USA, these patterns were consistent with a deeper and distinct sulfide depletion front, indicating that Re is not hosted in pyrite in the gray shale and sandstone weathering profiles in those river basins (Ghazi et al., 2022).

While Re is generally considered to remain stable in a dissolved form once released through weathering, a laboratory study found that the perrenate ion (ReO₄⁻) can form complexes with amine groups commonly found in natural organic matter (Kim et al., 2004). No direct evidence of Re interactions with natural organic matter in soil is available, although it has been hypothesized (Ogrič et al., 2023; Pierson-Wickmann et al., 2002).

2.1.2. Anthropogenic Rhenium Mobilization

Human activities accelerate the mobilization of Re into the surface environment, including soils and surface waters, through both mining activities and combustion of fossil fuels. The United States Geological Survey estimates that total worldwide Re production via mining and smelting was 53×10^6 g in 2019 (Polyak, 2021). Mine production of Re occurs primarily from porphyry copper (Cu) deposits, but is also sourced from stratabound Cu and sandstone uranium (U)-Cu deposits, and is currently concentrated in Chile, the United States, and Poland (John et al., 2017; Polyak, 2021). Rhenium is obtained as a byproduct during the production of molybdenum (Mo) as Re substitutes in molybdenite (MoS₂) (Barra et al., 2017; Barton et al., 2020); in turn, the Mo itself is generally a byproduct during the mining and production of Cu. During the roasting process, Re forms a flue gas (Re₂O₇, boiling point = 360°C), which is subsequently recovered as aqueous perrenic acid (Re₂O₇(H₂O)₂) via scrubbing (Anderson et al., 2013). Estimates of overall Re recovery during mining, concentration, and processing indicate that as much as 75% of the Re contained in ore may be lost to waste streams, predominantly tailings but also flue gases (Brainard, 2023). This implies that the 53×10^6 g yr⁻¹ of purified Re produced via mining may be accompanied by another 158×10^6 g yr⁻¹ (range 65×10^6 to 326×10^6 g yr⁻¹) of Re mobilized in the production process (Figure 1 and Table S2 in Supporting Information S1).

The relatively high mobility of Re and the non-reactive nature of perrenate ions in most environments at the Earth's surface lead to elevated Re concentrations in proximity to porphyry deposits, and in proximity to mining

and smelting activities (Barton et al., 2020). Groundwater near natural porphyry deposits in west-central Yukon and northern Chile display elevated Re concentrations (up to $3,800 \text{ pmol L}^{-1}$, and up to $165,000 \text{ pmol L}^{-1}$, respectively), which are $\sim 2\text{--}3$ orders of magnitude higher than what is observed in other worldwide groundwater (Kidder et al., 2022; Leybourne & Cameron, 2008) (Figure 2 and Table S1 in Supporting Information S1). Soils, plants, animal blood, and dairy products analyzed near a Mo ore mining and processing plant in the north Caucasus mountains showed elevated Re relative to nearby control areas, with cow milk showing a 47-fold greater Re content than cow milk from control areas (Ermakov et al., 2021). Larger regions that are downwind of known locations of Cu smelting also indicate anthropogenic mobilization of Re. Water from 283 small lakes in western Russia spanning a wide latitudinal transect had Re concentrations up to $11,300 \text{ pmol L}^{-1}$, far higher than concentrations in their local bedrock (Moiseenko et al., 2016). Similarly, high Re concentrations in lake sediments in eastern Canada reflect nearby smelter emissions, based on elevated Re/Al values observed in twentieth century sediments relative to those deposited in pre-industrial times (Chappaz et al., 2008). While coal combustion contributes to Re mobilization, the role of smelting activities is particularly important given that airborne particulate emissions from Cu smelters are extremely enriched in chalcophile elements, as compared to the element enrichment observed in coal combustion emissions (Small et al., 1981).

Fossil fuel combustion also accelerates mobilization of Re in the terrestrial environment. Coal samples display a wide range of Re concentrations, from 100 pg g^{-1} up to $3.4 \times 10^6 \text{ pg g}^{-1}$ ($n = 160$) (Figure 2 and Table S1 in Supporting Information S1). Elevated Re concentrations are usually associated with marine-influenced coals, such as those overlain by marine shale or carbonate strata (Baioumy et al., 2011; Dai et al., 2021; Tripathy et al., 2015). Terrestrial coals tend to contain less Re (Baioumy et al., 2011), in the same concentration range as terrestrial plants and also similar to the average continental crust value (e.g., Goswami et al., 2018) (Figure 2 and Table S1 in Supporting Information S1). The large range of values and limited data yield large uncertainty on the mobilization of Re via coal combustion. Using the 1st quartile and 3rd quartile Re concentration values for coals and combining with total global coal combustion (IEA, 2022) yields a potential coal-derived Re mobilization range of between 4.9×10^6 and $1,900 \times 10^6 \text{ g yr}^{-1}$ (Figure 1 and Table S2 in Supporting Information S1). Similar to coal, the available data on the Re content of petroleum and related samples (bitumen, crude oil, and oil sands) spans many orders of magnitude ($n = 71$) (Figure 2 and Table S2 in Supporting Information S1). Using the 1st quartile and 3rd quartile Re values for petroleum and combining with the global petroleum combustion (IEA, 2022) yields a potential petroleum-derived Re mobilization range of between 30×10^6 and $160 \times 10^6 \text{ g yr}^{-1}$ (Table S2 in Supporting Information S1).

2.1.3. Rhenium in Rivers

Dissolved Re in rivers occurs predominantly as an easily soluble perrhenate (ReO_4^-) oxyanion under prevailing redox and pH conditions encountered in most rivers (see Section 1). Perrhenate is so stable that filtered water samples can be stored unacidified for years without a decrease in concentration. Dissolved riverine Re concentrations vary by orders of magnitude, from $<1 \text{ pmol L}^{-1}$ (Rio Negro, Miller et al., 2011) that are indistinguishable from concentrations in rainwater (see Section 2.3), to 1240 pmol L^{-1} (South Platte River, USA; Miller et al., 2011). Concentration-discharge relationships for dissolved Re have been studied in a handful of locations globally including the Mackenzie River in Canada (Horan et al., 2019; Miller et al., 2011), the Whataroa River in the western Southern Alps, New Zealand (Horan et al., 2017), the Erlenbach and Vogelbach rivers in the Swiss Alps (Hilton et al., 2021); the East River in Colorado, USA (Hilton et al., 2021); and the Eel River and Umpqua River in the Pacific Northwest, USA (Ghazi et al., 2022). There are additional data available for some of the large rivers draining into the Arctic Ocean (Miller et al., 2011). Collectively, they exhibit average log-log slopes in between pure dilution (-1) and chemostatic behavior (0), indicating that increased runoff leads to higher riverine Re fluxes.

Miller et al. (2011) have shown that dissolved Re in global exorheic rivers (open systems where surface waters drain to the ocean) correlates well with dissolved sulfate concentrations, presumably because both elements are closely associated with sedimentary organic matter and related sulfides that are weathered under similar environmental conditions. Good positive correlations between Re and SO_4^{2-} were also observed in the left bank tributaries of the Orinoco River (Colodner et al., 1993) and the Yamuna River in India (Dalai et al., 2002). In tributaries to the Amazon River, contributions from evaporite weathering with high dissolved SO_4^{2-} and low Re concentrations weaken such correlations significantly (Colodner et al., 1993). However, Rahaman et al. (2012) observed that dissolved Re correlates much better with K^+ than with SO_4^{2-} in Indian Peninsular rivers. These authors use this

Table 2

Globally Averaged Actual and Natural Dissolved Rhenium Concentrations in Exorheic Rivers*

units →	Re	n =	Exorheic H ₂ O flux	Na	n =	K	n =	Mg	n =	Ca	n =	Cl	n =	SO ₄	n =	SiO ₂	n =
	pM		%	μM		μM		μM		μM		μM		μM		μM	
This review, modern	16±2	108	40	379	297	41	302	190	299	440	304	295	306	150	294	126	106
This review, pre-anthropogenic	10±1	108	40														
Miller et al. (2011), modern	16.5	38	37	270	34	38	34	193	34	470	34	190	31	190	35		
Miller et al. (2011), pre-anthropogenic	11.2	38	37														
Colodner et al. (1993), modern	2.3	4	24														
Livingstone (1963)				270		59		170		370		220		117			
Meybeck (1979), modern				313		35.8		150		367		233		120		173	
Meybeck (1979), pre-anthropogenic				224		33.2		138		334		162		85.9		173	
Meybeck and Helmer (1989), pre-anthropogenic				159		32		130		335		86		81.5		173	

Note. *Similarly averaged concentrations of major ions are also listed (from publications with Re concentration data and Gaillardet et al., 1995; Meybeck & Ragu, 2012; Tank et al., 2023), together with a few historic global averages for comparison. n represents the number of rivers used to determine the estimate. For Re, our new estimate represents 40% of the global exorheic water discharge, compared to 37% (Miller et al., 2011) and 24% (Colodner et al., 1993) in previous assessments.

correlation to propose a significantly lower global dissolved natural (i.e., pre-anthropogenic) Re concentration of only 3 pmol L⁻¹, a quarter of the value proposed by Miller et al. (2011) based on the Re-SO₄²⁻ correlation. Although the Rahaman et al. (2012) global average is much more similar to the ~2 pmol L⁻¹ estimate by Colodner et al. (1993), that estimate was based on only four large rivers representing 23% of the global river discharge. Colodner et al. (1993) did not correct that estimate for the “Amazon bias” (Meybeck, 1988) when scaling up from 23% of the global riverine discharge to the global runoff, thus allowing the Re poor (1.1 pmol L⁻¹) Amazon River to dominate the global budget.

In light of these conflicting findings, we have expanded the global river database (Peucker-Ehrenbrink, 2018) to include dissolved Re (n = 108) and major ions in rivers that drain directly to the ocean. This compilation includes data from the Orinoco (Colodner et al., 1993), Japanese rivers (Tagami & Uchida, 2008; Uchida & Tagami, 2008), Indian and East Asian rivers (Hilton et al., 2014; Rahaman et al., 2012), rivers in New Zealand (Horan et al., 2017), rivers draining into the Black Sea (Colodner et al., 1995) and some other smaller rivers along the North American West coast (Ghazi et al., 2022) that were not considered by Miller et al. (2011). New long-term water discharges of large Arctic rivers from Tank et al. (2023) replaced those used by Miller et al. (2011). We found no strong global correlation between Re and potassium (K⁺), but a notable positive one between Re and sulfate (SO₄²⁻). This finding is consistent with the observation by Tagami and Uchida (2008) that K⁺ is not among the dissolved elements in major Japanese rivers that exhibit correlations with Re with correlation coefficient (R) exceeding 0.4 (at p < 0.01). In the Tagami and Uchida (2008) data set, log-normalized correlations with SO₄²⁻ (R = 0.72) and Mo (R = 0.62) are the tightest of all elements investigated. Our expanded global exorheic river database (n = 2110) contains data on exorheic rivers from all large-scale drainage regions (Graham et al., 1999) except East Africa, the Baltic Sea and the Hudson Bay. Using the same regional averaging procedure that Miller et al. (2011) introduced to limit the “Amazon bias” (Meybeck, 1988) when upscaling to global discharge and fluxes, we calculate a global average dissolved Re concentration of 16 ± 2 pmol L⁻¹ based on almost 40% of exorheic river water discharge (Table 2). The greater number of available data for major ions means that the averages presented in Table 2 are based on almost 60% of the global exorheic river water discharge.

Due to the elevated Re concentrations in sedimentary rocks rich in organic matter (Section 2.1.1, Figure 2), weathering can elevate dissolved Re concentrations seen in rivers draining areas with those rocks (Colodner et al., 1993; Dalai et al., 2002; Miller, 2009; Pierson-Wickmann et al., 2002). However, elevated riverine Re concentrations can also be driven by industrial use and inadvertent release of Re as a byproduct of human activities. Some of the highest dissolved Re concentrations are related to mining activities, such as the Berkeley Pit porphyry Cu-Mo-Ag mine in Butte, Montana, USA (12,000–13,000 pmol L⁻¹) (Miller, 2009), mine waters at the Maldeota phosphorite mines in India (87 pmol L⁻¹) (Dalai et al., 2002) and the black-shale hosted Kupferschiefer mine at Mansfeld, Poland, with concentrations up to 37,000 pmol L⁻¹ Re (Miller, 2009). Miller (2009) suspects that high Re concentrations in the South Platte River in the western USA are caused by intense pumping and

subsequent evaporative enrichment of groundwater with high Re concentrations (Hodge et al., 1996; Leybourne & Cameron, 2008) that is used for irrigation in a dry interior climate (Miller, 2009). The 2018/9 time-series data on dissolved Re concentrations in the Yangtze River (Wang et al., 2024) indicate 1.5–3 times higher concentrations compared to those reported in Miller et al. (2011) on a sample collected in 2007. The increase in dissolved Re is accompanied by a similar increase in sodium (Na^+) and SO_4^{2-} , but not calcium (Ca^{2+}), concentrations. This increase may reflect significantly increased recent pollution that brackets in time the full operation of the Three Gorges Dam in 2012. Miller (2009) also reports periodic release from an unidentified Re source upstream of the Federal Dam at Troy on the Hudson River, USA. This transient pollution causes non-conservative mixing relationships in the salinity gradient of the Hudson River estuary that can occasionally lead to dissolved Re concentrations of up to 440 pmol L^{-1} in the freshwater end of the profile. Such concentrations exceed the Re concentration in seawater (40 pmol L^{-1}) by an order of magnitude, and that of uncontaminated Hudson River water by two orders of magnitude. Transient releases of Re in the freshwater portion of a salinity profile can mimic non-conservative release of Re from river sediments in the intermediate portion of an estuarine salinity profile.

In an effort to quantify the extent of anthropogenic Re pollution in rivers, we correct the modern average dissolved Re concentration in global rivers using the good correlation between dissolved Re and SO_4^{2-} (Miller et al., 2011). Meybeck (1979) and Meybeck and Helmer (1989) estimate that $\sim 30\%$ of the actual dissolved SO_4^{2-} concentrations in rivers are of anthropogenic origin. This estimate yields a pre-anthropogenic dissolved riverine Re concentration of about $10 \pm 1 \text{ pmol L}^{-1}$ (Table 2).

Rhenium is also transported by rivers in suspended particulate matter and bedload. Our compilation of river sediment data indicates that the Re concentration of river sediments essentially matches that of the UCC (median value 375 pg g^{-1} , 1st and 3rd quartiles $212\text{--}832 \text{ pg g}^{-1}$, $n = 296$, Figure 2 and Table S1 in Supporting Information S1). Combining our median Re concentration in river sediments with the global pre-anthropogenic sediment flux to the oceans (Svitski et al., 2005) yields a flux of $5 \times 10^6 \text{ g yr}^{-1}$ (estimated range of $3\text{--}12 \times 10^6 \text{ g yr}^{-1}$ using 1st and 3rd quartiles of Re concentration). Compared to the natural dissolved Re riverine flux of $62 \times 10^6 \text{ g yr}^{-1}$ (based on the natural concentration established above, combined with global river discharge (Berner & Berner, 2012), the natural dissolved Re flux exceeds the particulate flux by a factor of ~ 12 , making Re an element with one of the highest chemical mobility indices (cf. Figure 2 in Gaillardet et al., 2003).

2.2. Marine Environment

2.2.1. Rhenium Input in Near-Shore Environments

The estimated marine residence time of Re with respect to our new calculation of the pre-anthropogenic river input flux ($62 \times 10^6 \text{ g yr}^{-1}$, Table S3 in Supporting Information S1) is 1.6×10^5 years, given the Re concentration of seawater (Table S1 in Supporting Information S1) and ocean volume of $1.332 \times 10^{21} \text{ L}$ (Charette & Smith, 2010). This computation assumes that the dissolved Re transported by rivers to the ocean behaves conservatively. While the seawater Re end member is well established, the riverine end member is dynamic and dependent on the hydrographic conditions that control the natural mobilization of Re (e.g., Figure 3e). This could potentially cause the relationship between Re concentration and salinity along a river to estuary to ocean transect to deviate from a linear mixing line even if the behavior is conservative. Furthermore, given the high mobilization of Re from anthropogenic activities (Section 2.1.2), some rivers like the Mississippi and Hudson rivers in the USA, the Krka River in Croatia, and the Narmada and Tapi rivers in India have riverine Re concentrations greater than the global river average of $16 \pm 2 \text{ pmol L}^{-1}$ (Figures 3c–3f, and 3j). For multiple estuaries, a simple mixing behavior of Re between river water and ocean water is observed, for example, in the Mississippi River estuary in the USA, estuaries of the Mandovi and Hooghly rivers draining into the Arabian Sea, estuaries of the Narmada and Tapi rivers draining into the Bay of Bengal, and the Jiulong River estuary in the Taiwan Strait (Figures 3a–3f) (Ho et al., 2019; Miller, 2009; Rahaman & Singh, 2010; Zhu & Zheng, 2017). Data from other locations display more complicated mixing patterns (Figures 3g–3k), which could potentially lead to an overestimation or underestimation of the residence time of Re in the ocean, but the reasons for this disparity remain unclear. In the Amazon estuary, dissolved Re had near-conservative behavior except for three elevated dissolved Re concentrations at low salinity (Figure 3g). The authors suggest that either desorption of Re from suspended sediments or remobilization of Re from reduced phases in bottom sediments may be responsible (Colodner et al., 1993). Deviations from conservative behavior of dissolved Re were also observed in the Chilika Lagoon in India

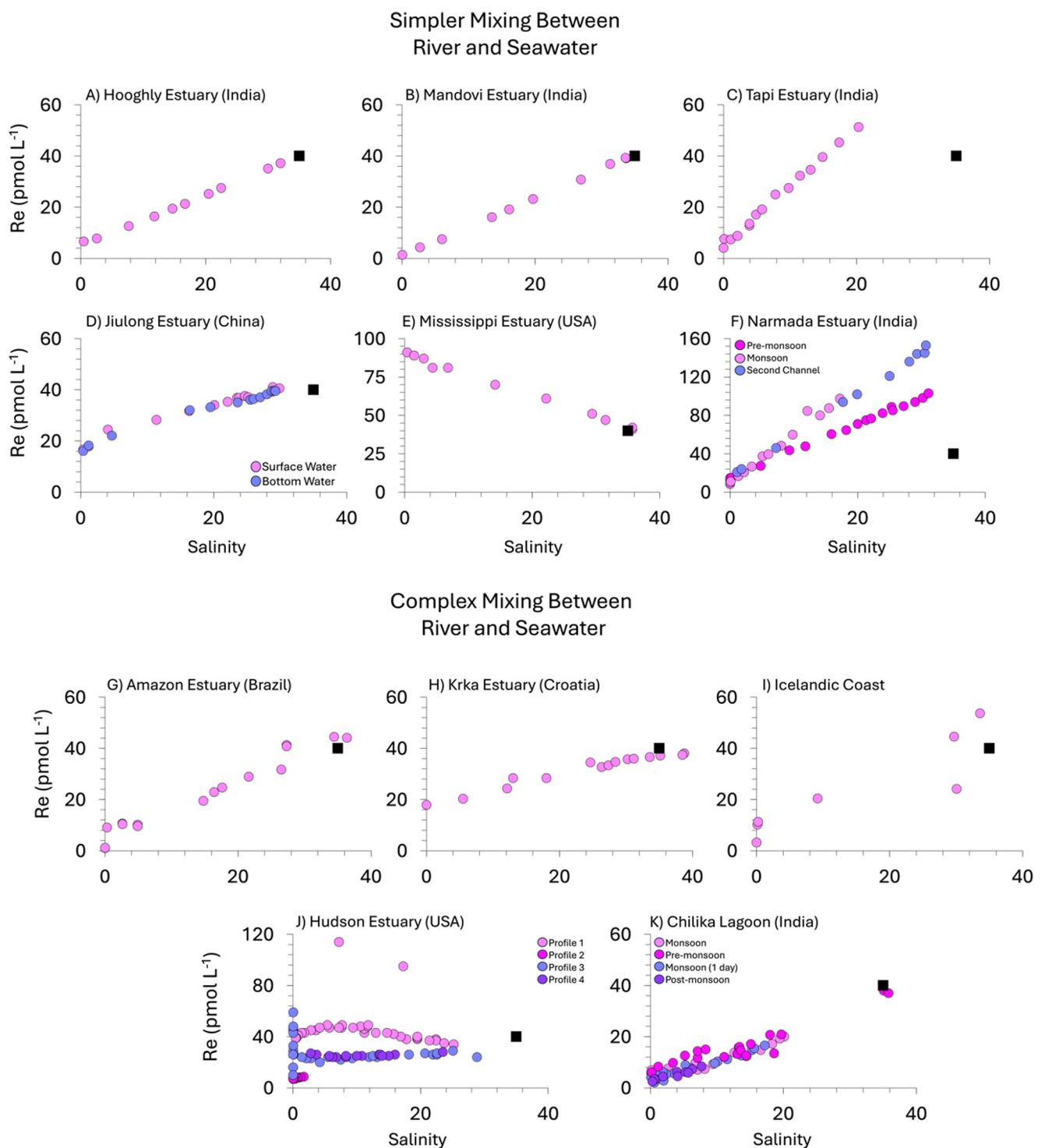


Figure 3. Dissolved Re and salinity data from various coastal regions worldwide. The black square represents the global Re seawater average. Data in the panels are reproduced from different studies. Panels (a, b, c, and f) represent data from (Rahaman & Singh, 2010). Panel (d) is data from (Zhu & Zheng, 2017). Panels (e, j) represent data from (Miller, 2009). Panel G is data from (Colodner et al., 1993). Panel (h) is data from (Nakić et al., 2021). Panel I is data from (Spronson et al., 2018). Panel (k) is data from (Danish et al., 2021).

(Figure 3k) and are attributed to processes such as clay adsorption and biological uptake by macroalgae (Danish et al., 2021). Biological uptake of Re by macroalgae has also been widely reported in other marine settings (Section 3.2), and evidence of this is seen in a salinity gradient along the Icelandic coastline (Figure 3i) (Spronson

et al., 2018). The Hudson River estuary has the greatest deviation from simple mixing (Figure 3j), which is mostly attributed to transient anthropogenic Re inputs in the highly industrialized area (Miller, 2009). Similarly, a small positive deviation from simple mixing in the Krka River was also attributed to anthropogenic inputs (Nacik et al., 2021). These findings highlight variations in behavior of Re during river-seawater mixing in coastal regions that may alter its true fluxes into the ocean. This underscores the need for more comprehensive research to accurately quantify both the ultimate fluxes of Re into the ocean and its residence time. Beyond the subtleties of the Re behavior reported for different types of water column, a recent study shows that the global Re budget is still being resolved (Hong et al., 2024). Their analysis suggests that the importance of reductive removal of Re in shelf sediments as a Re sink has been underestimated. This removal flux would likely vary through glacial-interglacial periods, depending on the exposure of the continental shelf.

Submarine groundwater discharge (SGD) is recognized as a significant source of chemical elements to the ocean, impacting their marine budgets (Burnett et al., 2006; Mayfield et al., 2021; Moore, 1997; Mulligan & Charlette, 2006; Schopka & Derry, 2012). In some instances, such as for barium (Ba) and vanadium (V), SGD may exceed riverine fluxes (Ho et al., 2019). However, individual estimates of elemental SGD fluxes are relatively limited, especially for Re. For certain elements, such as uranium, SGD is considered a net sink because seawater uranium is removed to anoxic sediments during seawater recirculation in coastal aquifers (Charette & Sholkovitz, 2006; Santos et al., 2011). Concentrations of chemical elements in SGD vary depending on the lithology of the aquifer, biogeochemical reactions, and redox conditions influencing solid-liquid exchange (Burnett et al., 2006). Consequently, the abundance of Re in coastal aquifers is primarily influenced by the weathering of organic matter-rich shales and anthropogenic sources. Given the redox-sensitive nature of Re, it is possible that SGD serves as a sink for this element from oceanic sources as observed for U. The only study available for determining the SGD-associated Re fluxes is from the subterranean estuary of the German North Sea (Reckhardt et al., 2017). In this study, the authors estimated a negative Re flux of $24.7 \text{ nmol day}^{-1} \text{ m}^{-2}$ along the shoreline, suggesting that SGD acts as a sink for Re. Therefore, further studies are necessary to refine estimations and elucidate the role played by SGD in controlling Re transport and cycling within coastal environments and marine budgets.

2.2.2. Rhenium Burial in Ocean Sediments

In the modern ocean, Re speciation is thought to be dominated by the geochemically inert perrhenate $\text{Re(VII)}\text{O}_4^-$ anion at a concentrations of $\sim 40 \text{ pmol L}^{-1}$ (Table S1 in Supporting Information S1). Within oxygenated pore-water, Re does not react directly with Al-, Fe-, Mn- oxyhydroxides, clay minerals, or recalcitrant particulate organic substances (Chappaz et al., 2008; Koide et al., 1986; Morford et al., 2009; Yamashita et al., 2007). Rhenium concentrations in oxic sediments are similar to those of the upper continental crust ($200\text{--}400 \text{ pg g}^{-1}$, Figure 2 and Table S1 in Supporting Information S1) (Poirier & Hillaire-Marcel, 2011; Wagner et al., 2013), signifying no significant authigenic enrichment under these conditions. The estimated Re burial rate in oxic environments ($\sim 84\%$ of total seafloor area) with large O_2 penetration depth below the sediment-water interface is $4.9 \times 10^6 \text{ g yr}^{-1}$ of Re (Sheen et al., 2018) (Figure 1 and Table S2 in Supporting Information S1).

Rhenium burial in reducing conditions is complex because several pathways are likely involved (Figure 4). Although the mechanisms involved in Re burial are unknown, they are widely believed to involve a reduction step from Re(VII) to Re(IV) . The Re precipitate most likely to form in ferruginous or manganous environments may be Re oxide ($\text{Re(IV)}\text{O}_{2(s)}$) as demonstrated by XANES data (Yamashita et al., 2007). Microbial experiments involving $\text{Re(VII)}\text{O}_4^-$ in the presence of Fe(III) reducing strains yielded no Re loss in one week, suggesting no direct or short term indirect microbial-mediated removal process (Dolor et al., 2009). A recent study by Kilber et al. (2024) reexamines the fate of oxidized Re in the presence of Fe(II) -bearing minerals, which are known as green rusts and are commonly observed following microbial Fe(III) reduction in the lacustrine or marine sediment. Using XANES measurements to characterize experimental samples, they found that Re may be reduced only when reacting with magnetite (Fe_3O_4). Clearly, additional research is needed in this area. Several authors (Dellwig et al., 2002; Nameroff et al., 2002; Sundby et al., 2004) hypothesized that Re sequestration is kinetically controlled, thus it is likely a slow reaction. Prior studies reported that Fe^{2+} associated with oxide surfaces may be a more potent reducing agent than free Fe^{2+} (Stumm & Sulzberger, 1992). For example, Fe^{2+} adsorbed to Fe oxides has been shown to promote reduction of $\text{Tc(VII)}\text{O}_4^-$ (Peretyazhko et al., 2008, 2012). A similar reduction pathway may exist for ReO_4^- . Organic polymers with functional groups do not react directly with $\text{Re(VII)}\text{O}_4^-$, but when a cation is added to the system (NH_4^+), Re can be adsorbed at the surface of these organic molecules via

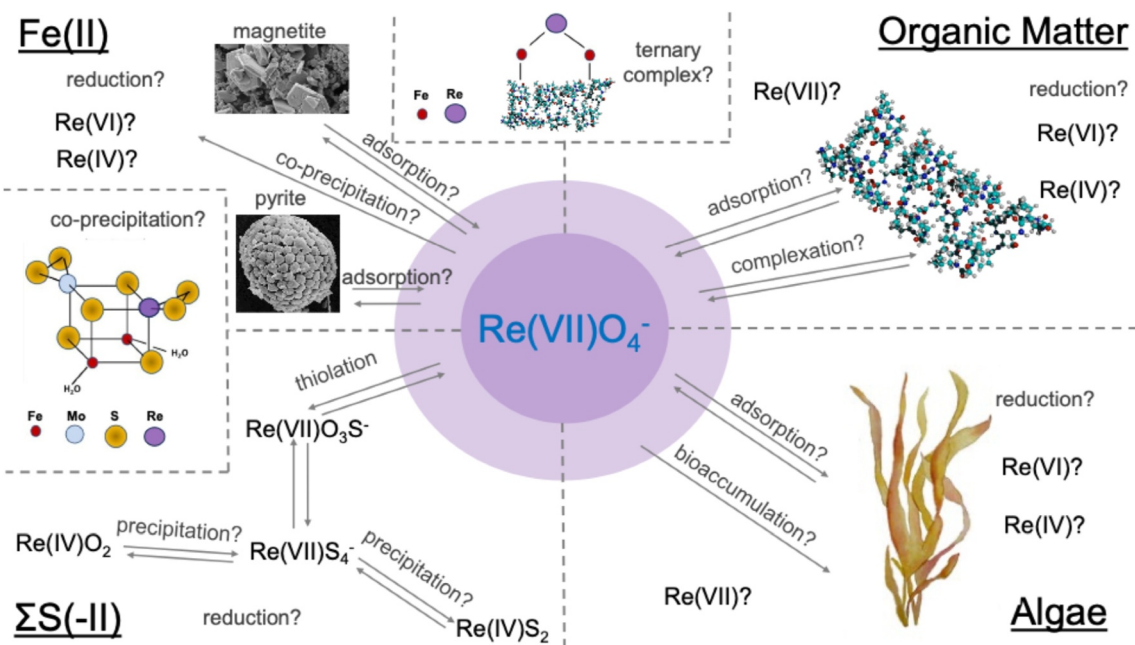


Figure 4. Schematic representation of the potential Re burial pathways. It is important to understand that several of the processes proposed for a given quadrant probably occur simultaneously.

an ion-pairing mechanism (Wu et al., 2016). Under ferruginous conditions, a similar reaction could occur with Fe^{2+} acting as a bridge between the anionic functional groups in natural organic matter and $\text{Re(VII)}\text{O}_4^-$ (Figure 4).

In the presence of sulfide, the perrhenate undergoes a transformation wherein the O atoms surrounding the Re can be substituted by S atoms, forming thioperrhenate species ($\text{Re(VII)}\text{O}_{4-x}\text{S}_x^-$) in a similar way to Mo (Vorlichek et al., 2015) (Figure 4). However, the sulfide concentrations required for this process to occur are far higher than those required for Mo (for an equivalent amount of Mo and Re) and the reaction kinetics are again slower (Helz & Dolor, 2012). Two thioperrhenates, $\text{Re(VII)}\text{O}_2\text{S}_2^-$ and $\text{Re(VII)}\text{OS}_3^-$, could not be detected during the experiment designed by Helz and Dolor (2012), possibly for kinetic reasons (meta-stable species). Rhenium profiles from sulfidic water columns and porewaters show a decrease in Re concentration as sulfide concentration increases, supporting the role played by sulfide in removing dissolved Re (Colodner et al., 1993; Helz, 2022; Morford et al., 2007) (Figure 5). This behavior is especially evident in the Black Sea, where the water column is devoid of oxygen below 85 m, which coincides with a decrease in the concentration of Re (Figure 5). The removal of Re from modern oceans is predominantly influenced by the suboxic areas (defined as O_2 penetration depth is less than 1 cm). Sheen et al. (2018) estimated a burial rate of $70 \times 10^6 \text{ g yr}^{-1}$ in suboxic regions ($\sim 5\%$ of seafloor) (Figure 1 and Table S2 in Supporting Information S1). Although covering only 0.1% of the total sea floor, anoxic sediments account for a Re burial rate of $5.2 \times 10^6 \text{ g yr}^{-1}$ (Sheen et al., 2018) (Figure 1 and Table S2 in Supporting Information S1).

Thermodynamic modeling of porewater Re profiles from a sulfidic lake suggested that Re could be buried in sediments as $\text{Re(IV)}\text{S}_2$ following a reduction step (Chappaz et al., 2008). Another Re-sulfide mineral has been proposed based on experimental work: Re_2S_7 (Dolor et al., 2009). Recently, a new Mo-Fe-S phase was synthesized and characterized (Vorlichek et al., 2018). It is possible that Re could either co-precipitate with this newly identified Mo phase or even form its own Re-Fe-S mineral (Helz, 2022; Helz & Dolor, 2012). Although the role of iron-sulfur mineral phases (pyrite and acid volatile sulfide) was discussed in previous studies, their contribution to Re removal to sediments has never been comprehensively studied. Sulfurized OM could also be involved during Re fixation, as demonstrated for Mo (Wagner et al., 2017) and as suggested by Helz and Adelson (2013). More studies of Re removal in shelf sediments are warranted.

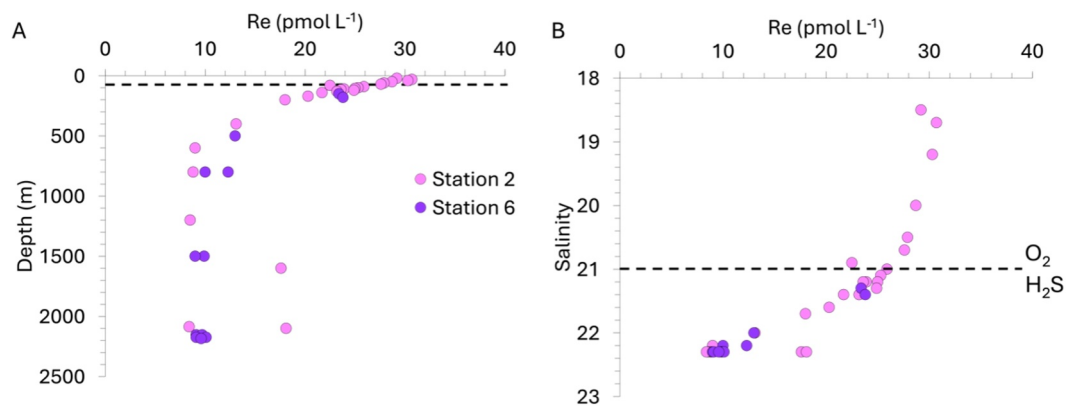


Figure 5. Rhenium removal in water columns and porewaters. Panels (a, b) represent data from (Colodner et al., 1993). (a) Dissolved Re concentrations in a vertical water column profile in the Black Sea. The horizontal line marks the water depth and salinity of the O_2 - H_2S interface at 85 m depth. (b) Dissolved Re concentrations versus salinity in the Black Sea.

2.2.3. Rhenium in Hydrothermal Fluids and Altered Oceanic Crust

Following the discovery of hydrothermal vents along the Galapagos Islands in 1977 (Corliss et al., 1979), exchanges between seawater and hydrothermal fluids along mid-ocean ridges have been recognized as important additional sinks or sources of elements from or to the ocean. Data representing the hydrothermal Re flux is sparse. Colodner et al. (1993) reported preliminary data for endmember hydrothermal fluids from the mid-Atlantic Ridge with Re concentrations below 0.1 pmol L^{-1} , consistent with almost complete loss of Re from seawater. Four hydrothermal fluid samples from the Manus Basin also showed lower Re concentrations ($0.65\text{--}14.4 \text{ pmol L}^{-1}$) than ambient seawater, which corroborates that hydrothermal circulation acts as a Re sink from the ocean (Miller et al., 2011). Unlike other oxyanions, there is evidence that Re does not coprecipitate with hydrothermal iron oxides (Ravizza et al., 1996; Schaller et al., 2000). Correcting the Manus Basin fluids to zero Mg concentrations, a widely used approach to extrapolate to pure hydrothermal fluids not contaminated by seawater (Mottl & Wheat, 1994; Von Damm et al., 1985), revealed that dissolved Re is more rapidly lost from circulating fluids than Mg (Miller et al., 2011).

Thermodynamic calculations aiming to simulate Re in hydrothermal systems suggested that the formation of Re-Cl complexes may promote high Re concentrations (Xiong et al., 2013; Xiong & Wood, 1999). However, in the presence of sulfide minerals, which are often present in hydrothermal systems, the formation of Re-Cl complexes is unlikely to occur because Re will precipitate with sulfide phases (Miller et al., 2011). Based on a very limited data set, a removal flux of $0.22 \times 10^6 \text{ g yr}^{-1}$ was proposed for high-temperature hydrothermal fluids (Miller et al., 2011) (Figure 1 and Table S2 in Supporting Information S1), which represents just 0.4% of the pre-anthropogenic riverine Re input. The complementary Re enrichment in hydrothermally altered oceanic crust has been observed in several locations, such as DSDP/ODP Sites 417/418 and 504 (Peucker-Ehrenbrink et al., 2003), ODP Sites 735B (Blusztajn et al., 2000) and 803 (Reisberg et al., 2008) and IODP Site U1527 (Ishida et al., 2022). The global Re flux into altered oceanic crust has been estimated at $6.5 \times 10^6 \text{ g yr}^{-1}$ (Reisberg et al., 2008). The fate of this Re in subduction zones is not well understood. Becker (2000) and Dale et al. (2007) argued that a significant fraction returns to the subarc mantle during slab dehydration and melting, possibly causing observed Re enrichment in olivine-hosted fluid inclusions in some undegassed arc-type volcanic glasses and rocks (Sun et al., 2003). In contrast, Xue and Li (2022) present experimental evidence against slab melting being a significant return flux to the sub-arc mantle and instead argue that between 60 and $230 \times 10^6 \text{ g Re yr}^{-1}$ are subducted into the deep mantle (Figure 1 and Table S2 in Supporting Information S1).

2.3. Atmosphere

2.3.1. Inputs of Rhenium to the Atmosphere

While undegassed mantle-derived magmas are generally enriched in Re over typical mantle concentrations owing to the moderately incompatible behavior of Re during mantle melting, degassing results in partial loss. A sequence of submarine to subaerial lava recovered from the HSDP2 Mauna Kea drillcore shows that degassing

during subaerial eruptions can cause lava to lose at least 80% of their initial Re inventory (Lassiter, 2003). Volcanic emissions of Re, though currently poorly constrained, can therefore be an important component of the global Re budget. Concentrations of many trace metals, including Re, are elevated in volcanic emissions relative to corresponding lava and relative to background air, making them of particular interest to the biogeochemical budgets of trace metals (Hinkley et al., 1999; Zelenski et al., 2013). Rhenium concentrations have been measured in volcanic aerosols and reactive gases from ocean island settings (Mauna Loa and Kilauea in Hawaii), from subduction zone volcanoes (Kudryavy in the Kurile arc and Etna in Italy), and from a continental rift setting (Erta Ale in Ethiopia) (Aiuppa et al., 2003; Hinkley et al., 1999; Krähenbühl et al., 1992; Mather et al., 2012; Taran et al., 1995; Yudovskaya et al., 2008; Zelenski et al., 2013). Flux data from the Kilauea volcano of $44\text{--}166\text{ g Re}$ per day imply that, when scaled, volcanic Re emissions likely outweigh other natural fluxes of Re to the atmosphere (Mather et al., 2012). Enrichment of Re relative to magmatic concentrations was particularly elevated ($3.5\text{--}8 \times 10^5$) in gas condensates from the subduction zone Kudryavy volcano (Yudovskaya et al., 2008). Exceptionally high Re enrichments have also been observed in volcanic gas condensates from Merapi volcano in Java, Momotombo in Nicaragua, and Mt. St. Helens, USA (Bernard et al., 1990). An estimate of Re volcanic emissions can be made based on ratios using simultaneously sampled Re and sulfur data, together with overall volcanic sulfur fluxes. Combining the worldwide SO_2 emission from volcanoes of $13 \times 10^{12}\text{ g yr}^{-1}$, (including both quiescent degassing and explosive emissions) (Bluth et al., 1993) with the range of Re/SO_2 ratios observed in gaseous emissions from Etna, Kilauea, Kudryavy, and Erta Ale, the estimated range of global volcanic Re emissions is $1.6\text{--}82 \times 10^6\text{ g yr}^{-1}$ (Figure 1 and Table S2 in Supporting Information S1).

Most other natural fluxes of Re into the atmosphere are relatively small. Rhenium emissions in the form of desert dust are uncertain because of limited data on the Re content of dust. However, using the median value for loess of 176 pg g^{-1} Re ($n = 68$) (Figure 2 and Data Set S1), combined with an estimated global dust flux of $1.5\text{--}2.6 \times 10^{15}\text{ g yr}^{-1}$ (Cakmur et al., 2006) yields an estimated range of $0.26\text{--}0.46 \times 10^6\text{ g yr}^{-1}$ of Re mobilized (Figure 1 and Data Set S2). Unlike certain trace metals such as Mo, which are enriched in fertilizers (Wong et al., 2021), Re is unlikely to have enhanced concentrations in agricultural soils, so agricultural dust mobilization is not expected to significantly impact Re fluxes via dust. Cosmic dust inputs are on the order of $30,000 \times 10^6\text{ g yr}^{-1}$ (Love & Brownlee, 1993; Peucker-Ehrenbrink & Ravizza, 2000). When combined with the abundance of Re in meteorites (Anders & Grevesse, 1989), the cosmic dust flux of Re is about $0.001 \times 10^6\text{ g yr}^{-1}$. A similar calculation for sea spray aerosols also yields a small flux of Re of $0.03 \times 10^6\text{ g yr}^{-1}$ (Klee & Graedel, 2004) (Figure 1 and Table S2 in Supporting Information S1).

The anthropogenic flux of Re to the atmosphere is not well-constrained by direct measurements. Based on observed surface Re enrichment evident in soils, biota and surface waters downwind from smelting and fossil fuel burning, we infer that anthropogenic Re inputs to the atmosphere may be substantial (e.g., Chappaz et al., 2008; Moiseenko et al., 2016; Ogric et al., 2023; Prouty et al., 2014). One long term record of weekly atmospheric particulate samples from 1964 to 2010 collected in northern Finland found that more than 70% of the Re in the filter-captured particles was water soluble, and that there was a significant decreasing trend in Re content over time (Laing et al., 2014a, 2014b). This suggests that Eurasian emissions of Re to the atmosphere from fossil fuel combustion and smelting have decreased in recent decades, although the relative influence of changes in industrial practices such as scrubbing of flue gases and particulates versus changes in production is not known.

2.3.2. Rhenium in Precipitation

Only a limited number of analyses of Re in precipitation have been made (Table S1 in Supporting Information S1). Precipitation samples from central Pennsylvania and the eastern coast of Massachusetts in the U.S., both sites that are downwind of significant human activity, averaged 1.3 pmol L^{-1} Re, with a range of $0.3\text{--}5.9\text{ pmol L}^{-1}$ Re ($n = 24$) (Miller et al., 2011; Ogric et al., 2023). In contrast, a small number of samples from relatively remote sites in the western U.S., the Southern Alps of New Zealand, and the Peruvian Andes had lower Re concentrations averaging 0.12 pmol L^{-1} , (range $0.03\text{--}0.20\text{ pmol L}^{-1}$, $n = 4$) (Dellinger et al., 2023; Ghazi et al., 2022; Horan et al., 2017). Using the lower value of 0.03 pmol L^{-1} and the upper value of 5.9 pmol L^{-1} and $1.13 \times 10^{17}\text{ L yr}^{-1}$ of global precipitation (Trenberth et al., 2007) yields a preliminary global estimate of between 2 and $534 \times 10^6\text{ g yr}^{-1}$ for global deposition of Re (Figure 1 and Table S1 in Supporting Information S1).

3. Rhenium in Biota

3.1. Rhenium in the Terrestrial Biosphere

Rhenium plays no known role in biology and is not among the trace elements that are essential for living organisms. A limited number of Re measurements on terrestrial plant samples have been reported with a median value of 344 pg g^{-1} ($n = 22$), which is very similar to the value for the upper continental crust (Figure 2 and Data Set S1). Of the available data, mosses and lichens from northern Sweden had lower Re concentrations ($<100 \text{ pg g}^{-1}$) as compared to nearby shrubs and tree foliage (Rodushkin et al., 2007). Higher Re concentrations ($>1,000 \text{ pg g}^{-1}$) were observed in grass samples from near Moscow, Russia, and in the European Beech leaves certified reference material (Ermakov et al., 2021; Kučera et al., 2006). Plant uptake of perrhenate ions is presumed to take place via anion transporters on root surfaces, and Re is subsequently preferentially transported to aboveground plant tissues (Bozhkov et al., 2007; He et al., 2018; Tagami & Uchida, 2004). Extraction tests suggest that Re remains in perrhenate species form in plant tissue and is stored in leaf cell vacuoles (Borisova et al., 2010; Tzvetkova et al., 2021). Almost no information is available on Re toxicity to organisms, although a plant study found increasingly stunted plant growth and photosynthesis at high soil Re contents 7–8 orders of magnitude larger than the crustal abundance (Novo et al., 2018).

Elevated Re concentrations in plant and animal materials may be used as biomonitoring to indicate underlying Re enrichments, which may occur in the vicinity of ore deposits and metal smelting operations (Borisova et al., 2010; Ermakov et al., 2021) or bitumen deposits (La Flèche et al., 2021). Given the extremely low abundance of Re in the Earth's crust and its high economic value (1000 USD per kg in 2022) (US Geological Survey, 2023), a number of studies have investigated the possibility that biologically concentrating Re via phytoextraction may be an economically viable means of producing Re in environments near mine tailings or smelting operations or in coal fly ash-amended soils (He et al., 2018; Novo et al., 2018; Tabasi et al., 2018; Tzvetkova et al., 2021).

3.2. Rhenium in the Marine Biosphere

Rhenium also plays no known biological role in the oceans (Morel et al., 2006). Dissolved Re has a conservative-type vertical concentration profile as opposed to the nutrient-type profiles that are observed for metals such as Cu and Ni that are essential micronutrients (Anbar et al., 1992; Colodner et al., 1993). Rhenium is not scavenged by marine particulate organic matter (Prouty et al., 2014), and there is no microbial fixation of Re in marine sediments, with sediment Re sequestration instead being driven by abiotic processes under reducing conditions (Section 2.2) (Dolor et al., 2009). Some marine biota have low Re concentrations, such as zooplankton from the Gulf of Mexico ($0.2\text{--}1.4 \text{ pg g}^{-1}$) (Prouty et al., 2014) and marine cyanobacteria (*Microcoleus chthonoplastes*) (83 pg g^{-1}) (Miller, 2004). In contrast, however, some marine macroalgae actively take up and concentrate Re (Racionero-Gómez et al., 2016; Sproson et al., 2018; Yang, 1991).

Brown algae in particular show large accumulations of Re relative to seawater (median value $22,500 \text{ pg g}^{-1}$, range $80\text{--}138,000 \text{ pg g}^{-1}$, $n = 74$), and greater accumulations than what has been observed in green or red algae (median value 600 pg g^{-1} , range 20 to $16,000 \text{ pg g}^{-1}$, $n = 28$) (Figure 2 and Table S1 in Supporting Information S1). Relative to seawater, the enrichment factor for Re in brown algae can be in the hundreds or thousands (Kučera et al., 2006). Rhenium accumulation is thought to be a coincidental byproduct of their iodine uptake (Van Sande et al., 2003). Macrophyte Re enrichment together with their biomass abundance observed in some coastal systems imply that macroalgae may constitute a significant coastal sink of Re (Danish et al., 2021). Variations in Re concentrations observed in brown algae may reflect the age of the particular seaweed sample (Mas et al., 2005), and in some cases they are correlated with variations in the dissolved Re concentrations of the water they live in (Sproson et al., 2018). The enrichment of Re in certain macroalgae is also evident in the paleo record of marine sedimentary rocks such as Devonian algal laminites and carbonate reefs (Miller, 2004; Saintilan et al., 2023). Uptake of Re in brown algae is active and unidirectional, as opposed to occurring via passive diffusion (Racionero-Gómez et al., 2016). Rhenium uptake in macroalgae is also of interest because it serves as an analog for Tc uptake; Tc also forms a stable oxyanion in water (TcO_4^-) and is monitored as a tracer of nuclear waste contamination in the environment (Racionero-Gómez et al., 2016). The exact nature of Re storage in macroalgae is not well understood but is suggested to occur in cellular membrane proteins (Melián et al., 2000; Xiong et al., 2013).

4. Biogeochemical Applications

4.1. Rhenium Enrichments as a Paleo-Redox Proxy

Changes in oceanic oxygen concentrations have drastically impacted the evolution of life and global biogeochemical cycles (Lyons et al., 2021). Today, dead zones (hypoxia) threaten 90% of marine coastal zones as a result of anthropogenically induced eutrophication and global warming, which contribute to the expansion of oxygen minimum zones in the modern oceans (Schmidtke et al., 2017). Quantifying how, when, and by how much oxygen levels increased in the ancient ocean, and co-evolved with life through geologic time, is an important challenge. Given that direct measurements of oxygen in ancient systems are impossible, suitable geochemical paleo-redox proxies measured in sedimentary records are needed. Ancient and current redox conditions prevailing in any aquatic system should be defined by the predominant electron acceptor during the oxidation of the organic matter (Hlohowskyj et al., 2021). For example, manganous, ferruginous and sulfidic are associated with the redox couples Mn(IV)/Mn(II), Fe(III)/Fe(II) and S(VI)/S(-II), respectively. High Mo enrichment in reducing settings are often linked to sulfidic conditions (Scott & Lyons, 2012). Rhenium often displays enrichment while Mo remains in crustal abundance. Such disparities in enrichment are clear in downcore profiles where Re is removed at depths shallower than Mo, where measurable sulfide is not present, at similar depths as the reduction and formation of solid-phase Fe and U (Morford et al., 2005, 2012). Crusius et al. (1996) suggested that Re could be used as an indicator of suboxic conditions. The Re/Mo ratio in reducing settings can refine the characterization of the redox conditions prevailing at the time of the deposition, particularly manganous and ferruginous redox conditions (Helz, 2022). The most elevated levels of Re are found in euxinic settings, where concentrations of several $\mu\text{g g}^{-1}$ constitute the highest level of enrichment among trace elements found in black shales (Brumsack, 2006). Paleoredox reconstructions using Re concentrations or concentration ratios may soon be complemented by the use of natural variations in the fractional abundance of Re isotopes (see Section 4.3.)

4.2. Geologic Respiration Using Dissolved Rhenium

On geologic timescales, the amount of CO_2 released from the oxidation of OC_{petro} (also known as geologic respiration) is uncertain but is thought to be similar in order of magnitude to volcanic degassing (Berner, 2006; Hilton & West, 2020). In Section 2.1.1, we discuss the distribution of Re in different rock types, and approaches to identifying the specific phase associations of Re within rocks. Much of the effort to understand which phases Re is associated with has been driven by interest in using Re as a tracer to construct the geologic respiration part of the global C budget.

Rhenium flux measurements can be used to estimate the OC_{petro} oxidation during weathering on Earth's surface environment. Regional studies have used the Re proxy to calculate OC_{petro} oxidation fluxes in the Yamuna and Ganga basins in the Himalaya, mountain belts in Taiwan and New Zealand, small alpine catchments in Switzerland and Colorado, the Mackenzie River basin, and the Rio Madre de Dios basin in the Andes and Amazon foreland-floodplain (Dalai et al., 2002; Dellinger et al., 2023; Hilton et al., 2014, 2021; Horan et al., 2017, 2019). Recently, the Re proxy has been used to attempt a first global assessment of OC_{petro} oxidation (Zondervan et al., 2023). This work builds on these prior studies and calculates a global OC_{petro} oxidation rate of 68 Mt C yr^{-1} (range of $62\text{--}86 \text{ Mt C yr}^{-1}$), which rivals in magnitude a major carbon sink via the global silicate weathering flux ($94\text{--}143 \text{ Mt C yr}^{-1}$), especially during periods of increased tectonic uplift. Using a global data-driven model approach, Zondervan et al. (2023) used dissolved riverine Re concentrations corrected to Re specifically associated with OC_{petro} using the ion ratio approach (see Section 2.1.1). They combine dissolved Re with Re/C_{org} relationships in crustal rocks to estimate the fraction of petrogenic organic carbon that is respiration upon erosion of OC-bearing rocks. They use global lithologic maps to determine OC_{petro} abundance in source rocks, compute denudation rates based on digital elevation models and utilize oxidative weathering rates to estimate the global flux of OC_{petro} . This finding, which relies on the Re tracer, refines our understanding of how orogenic periods during Earth history affect atmospheric CO_2 concentrations.

4.3. Terrestrial Weathering Using Stable Rhenium Isotopes

Redox processes that shape biogeochemical cycling of Re at the Earth's surface have the potential to fractionate ^{185}Re and ^{187}Re during initial burial, subsequent diagenesis (Colodner et al., 1993; Crusius & Thomson, 2000) and eventual re-oxidation, potentially leaving an isotopic record of past redox conditions (Miller et al., 2009, 2015). The change in the redox state of Re can induce fractionation between ^{187}Re and ^{185}Re by more than 1%

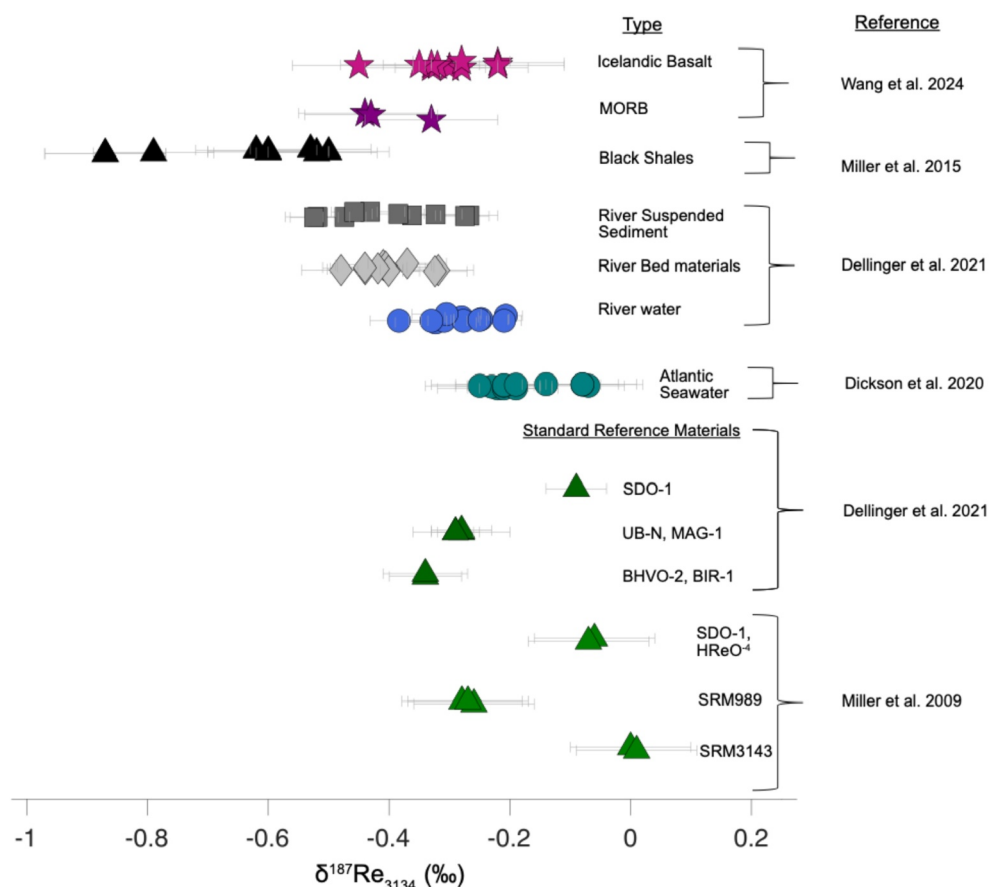


Figure 6. Composition of measured $\delta^{187}\text{Re}$ values in different terrestrial materials. Previously measured samples were replotted from their original sources. The igneous rocks include Icelandic Basalt (pink star) and mid-ocean ridge basalt (MORB) (purple star) first published in (Wang, Dickson, et al., 2024), while black shales are designated by black triangles and published in (Miller et al., 2015). The river samples, including suspended sediment (gray square), riverbed material (gray diamond), and river water (blue circle), are from (Dellinger et al., 2021). Atlantic seawater (teal circles) was first reported in (Dickson et al., 2020). Standard reference materials (green triangles) were replotted from two different studies (Dellinger et al., 2021; Miller et al., 2009). Multiple USGS rock standard reference materials have been reported, including Devonian Ohio shale (SDO-1), MAG-1 is a marine sedimentary mud, UB-N is representative of Earth's upper mantle, BHVO-2 is a Hawaiian basalt, and BIR-1 is an Icelandic basalt, while SRM989 and SRM3143 are NIST isotopic Re standard reference materials.

(Figure 6). The stable Re isotope system thus complements the stable U and Mo isotope systems, which have both been used as indicators of global changes in redox conditions (Severmann & Anbar, 2009).

At the beginning of the development of the stable Re isotope system, NIST SRM 989 was the agreed upon standard reference material (Brand et al., 2014). However, the supply of SRM 989 is exhausted and the community has shifted to NIST SRM 3143 as the normalizing standard reference material (Brand et al., 2014). Within this paper, we convert and discuss all isotope values $\delta^{187}\text{Re}$ (see Table 1) relative to the NIST SRM 3143 Re solution. The variability found to date spans from -0.97 to $0.09\text{\textperthousand}$ (Figure 6) (Dellinger et al., 2020, 2021; Dickson et al., 2020; Wang et al., 2024).

Despite the potential of this tool, it is in the early stages of applications and only a handful of different earth materials have been measured, published in only seven studies to date (Figure 6). One of these studies is beyond the scope of this paper because it focuses on extraterrestrial samples (Liu et al., 2017). Natural Re isotope fractionation was initially observed and quantified in a black shale weathering profile in New Albany, KY (Miller, 2009; Miller et al., 2015). The profile exhibits a $-0.3\text{\textperthousand}$ difference in $\delta^{187}\text{Re}$ between the unweathered black shales and the residual weathered material, with an incidental loss of 75% of the OC and a 100-fold decrease in Re concentration, indicating that the heavier ^{187}Re isotope is preferentially lost to the dissolved phase during

oxidative weathering and loss of the OC_{petro}. This finding formed the basis of the Re isotope proxy's potential use as a tracer of the oxidation of petrogenic organic carbon. The initial observation was corroborated in the Mackenzie River basin where dissolved Re has a heavier Re isotopic signature ($-0.28 \pm 0.05\text{\textperthousand}$; $n = 11$) relative to bedload ($-0.40 \pm 0.05\text{\textperthousand}$, $n = 10$) and suspended sediments ($-0.40 \pm 0.05\text{\textperthousand}$; $n = 10$) (Dellinger et al., 2021). The $\sim 0.30\text{\textperthousand}$ range in river water composition may indicate mixtures of isotopically distinct sources that include OC_{petro}, sulfides, and silicate hosted Re. Mackenzie River water is isotopically lighter than modern Atlantic seawater ($\delta^{187}\text{Re}$ of $-0.17\text{\textperthousand}$ (Dickson et al., 2020) by $\sim 0.12\text{\textperthousand}$, confirming the prediction that continental input of $\delta^{187}\text{Re}$ should be lighter than seawater because marine sinks should preferentially incorporate ^{185}Re (Dellinger et al., 2021; Dickson et al., 2020; Miller et al., 2015). At this time, there is only one data point for the isotopic composition of Re in modern marine sediments, which is the MAG-1 marine mud reference material, with a $\delta^{187}\text{Re}$ of $-0.27\text{\textperthousand}$, which is $\sim 0.1\text{\textperthousand}$ lighter than seawater (Dellinge et al., 2020). However, the composition of Re in such sediments can be predicted with ab initio calculations (Miller et al., 2015) together with the composition of modern seawater perrhenate (Dickson et al., 2020). These calculations predict that modern sediments should be fractionated toward lower $\delta^{187}\text{Re}$ values by up to $-1.5\text{\textperthousand}$ relative to the $\delta^{187}\text{Re}$ of seawater. Marine sediments are therefore expected to display a significant range in composition spanning from $-0.3\text{\textperthousand}$ to $-1.5\text{\textperthousand}$ depending on the Re speciation resulting from the complex burial processes involved.

Understanding how the Re isotopes behave in magmatic systems is essential for their use in quantifying the redox state of Earth's surface, OC_{petro} oxidation, and to assess the global isotope mass balance of Re. Thus far, studies of Re isotopes in igneous rocks are limited to meteorites (Liu et al., 2017), standard reference materials (Dellinger et al., 2020) and the Hekla volcanic sequence in Iceland (Wang et al., 2024) that may serve as a much-needed terrestrial baseline for $\delta^{187}\text{Re}$ of $-0.33 \pm 0.13\text{\textperthousand}$ (2 s.d., $n = 14$). A study of the Hekla volcanic sequence found that Re concentrations decrease during magmatic evolution from 1400 pg g^{-1} to 20 pg g^{-1} as Re is incorporated into magnetite. However, Re isotopes are not detectably fractionated during this process. Wang et al. conclude that un-degassed and unaltered basaltic rocks can be used to infer Re isotopic composition of their source. However, if magmatic systems have undergone degassing or hydrothermal alteration, Re isotopes may well fractionate even in high temperature systems. This study lends valuable insights into how Re may behave in other magmatic and high temperature systems and helps constrain the isotopic composition of the silicate end-member. Standard reference materials from high temperature magmatic systems, such as BHVO-2 (Hawaiian basalt), BIR-1 (Icelandic basalt) and BCR-2 (Columbia River basalt), show a limited range in $\delta^{187}\text{Re}$ (-0.44 to $-0.33\text{\textperthousand}$) and overlap with a carbonaceous chondrite value ($-0.29 \pm 0.03\text{\textperthousand}$) (Dellinger et al., 2020).

4.4. Tracing Anthropogenic Rhenium Pollution Using Dissolved Rhenium

Comparison of natural and anthropogenic elemental fluxes reveals the degree of human imprint on elemental cycling. The expanded data set summarized in this paper indicates that Re mobilization at the Earth's surface is significantly elevated by human activities. Assessments of natural versus anthropogenic flows for a wide suite of elements across the periodic table have found that Re is one of the most highly human-impacted elements (Klee & Graedel, 2004) although less data was available previously. A comparison between Re mobilized via coal combustion versus weathering release by Bertine and Goldberg (1971) estimated that coal combustion released 7 times as much Re. More recently, Sen and Peucker-Ehrenbrink (2012) found that human fluxes of Re are ~ 3 times higher than the natural fluxes, a factor which exceeds that of most other metals, including, for example, vanadium, mercury, and lead (Schlesinger et al., 2017). The new fluxes presented in this paper amount to a factor of about three to four times higher for the sum of human fluxes relative to the sum of natural fluxes. The imprint of these anthropogenic fluxes on Earth's surface Re cycle is evident at both local and regional scales in the atmosphere, soils, surface waters, biota, and lake sediments (Chappaz et al., 2008; Ermakov et al., 2021; Fritsche & Meisel, 2004; Laing et al., 2014a, 2014b; Moiseenko et al., 2016; Ogric et al., 2023; Prouty et al., 2014).

The fate of anthropogenically mobilized Re is not well known. In particular, data on the fate of Re associated with mining waste streams are lacking, although large losses are estimated during the mining, concentrating, and processing stages (Brainard, 2023). In the case of coal combustion, large waste streams of residual coal ash (both bottom ash and fly ash) are generated. These residues have multiple fates, including impoundment in landfills or ash ponds, use as agricultural soil amendments, and use in cement. Some studies have highlighted that coal ash may even serve as a potentially economically viable source of Re (Dai et al., 2015; He et al., 2018). Before modern air pollution control regulations in industrialized countries, fly ash became airborne particulate emissions. A long-term study of airborne particulates in Finland indicates a decline in atmospheric Re between 1980 and 2012,

although the relative impact of smelter operations, overall Eurasian coal combustion rates, and the implementation of pollution control measures is not resolved (Laing et al., 2014b). Dissolved Re in river water integrates watershed Re mobilization and thus provides a particularly useful tracer for anthropogenically enhanced Re mobilization. Even larger anthropogenic contributions to riverine dissolved Re fluxes of >90% have been inferred in a small catchment in central Pennsylvania, USA, and in the large Yangtze River basin (Ogrič et al., 2023; Wang et al., 2024). Only one long-term biogenic record of Re is available, in the form a proteinaceous deep sea black coral from the Gulf of Mexico (Prouty et al., 2014). Interestingly, these samples had very high Re concentrations, ranging from 1×10^6 pg g⁻¹ in the center to over 14×10^6 pg g⁻¹ in the outer part of the coral's skeletal growth, with a striking increase in Re concentrations taking place in the time period representing the last 150–200 years, coincident with the expansion of coal production in the Mississippi River watershed, and also coincident with a 4 fold increase in Mississippi River SO₄²⁻ fluxes (Killingsworth & Bao, 2015). Taken together, the limited available records indicate that environmental Re concentrations are a particularly sensitive tracer for human activities.

5. Conclusion

Historically, Re was an enigmatic element due to its rarity. With advances in analytical methods for measuring Re and its isotopes, the application of Re to biogeochemical problems has proliferated. Rhenium is now used to advance the fundamental understanding of Earth's oxygen and carbon cycles, both modern and through geologic time.

Our calculations of the important sources and sinks of Re through Earth's surface reservoirs highlight the degree of anthropogenic perturbation to the natural Re cycle. Enhanced Re fluxes stem from mining, coal combustion, and petroleum combustion, and this anthropogenic mobilization of Re requires careful attention when applying Re as a tracer of rock weathering, riverine, or estuarine processes. Natural transport of dissolved and particulate Re is dominated by continental weathering and volcanic degassing. Several potential sources of Re in the terrestrial and marine environment remain quite understudied and unconstrained, including submarine hydrothermal venting, magmatic degassing, and SGD. The dominant pathway of Re removal is in marine sediments. Removal fluxes in the oceans are dominated by those in suboxic/euxinic and anoxic conditions, despite their small area on the seafloor. Another important potential sink of Re is subduction, but this remains poorly constrained. The fluxes provided in this review are a potential starting point for future studies to constrain these especially unknown sources and sinks. In addition to the use of Re as a chronometer in deep geologic time, Re is also relevant to understanding Earth surface processes, including its value as a redox tracer, a tracer of anthropogenic pollution, and a tracer for oxidation of petrogenic organic carbon, an important flux in the long term carbon cycle.

Data Availability Statement

All of the data used in this synthesis are available in the citations in the manuscript and in supplementary tables, available in an online repository at Ghazi et al., 2024.

References

Aiuppa, A., Dongarrà, G., Valenza, M., Federico, C., & Pecoraino, G. (2003). Degassing of trace volatile metals during the 2001 eruption of Etna. *Geophysical Monograph-American Geophysical Union*, 139, 41–54. <https://doi.org/10.1029/139gm03>

Allègre, C. J., & Luck, J.-M. (1980). Osmium isotopes as petrogenetic and geological tracers. *Earth and Planetary Science Letters*, 48(1), 148–154. [https://doi.org/10.1016/0012-821x\(80\)90177-6](https://doi.org/10.1016/0012-821x(80)90177-6)

Anbar, A. D., Creaser, R. A., Papanastassiou, D. A., & Wasserburg, G. J. (1992). Rhenium in seawater: Confirmation of generally conservative behavior. *Geochimica et Cosmochimica Acta*, 56(11), 4099–4103. [https://doi.org/10.1016/0016-7037\(92\)90021-A](https://doi.org/10.1016/0016-7037(92)90021-A)

Anbar, A. D., Duan, Y., Lyons, T. W., Arnold, G. L., Kendall, B., Creaser, R. A., et al. (2007). A whiff of oxygen before the great oxidation event? *Science*, 317(5846), 1903–1906. <https://doi.org/10.1126/science.1140325>

Anders, E., & Grevesse, N. (1989). Abundances of the elements: Meteoritic and solar. *Geochimica et Cosmochimica Acta*, 53(1), 197–214. [https://doi.org/10.1016/0016-7037\(89\)90286-x](https://doi.org/10.1016/0016-7037(89)90286-x)

Anderson, C. D., Taylor, P. R., & Anderson, C. G. (2013). Extractive metallurgy of rhenium: A review. *Mining, Metallurgy & Exploration*, 30(1), 59–73. <https://doi.org/10.1007/bf03402342>

Baioumy, H. M., Eglinton, L. B., & Peucker-Ehrenbrink, B. (2011). Rhenium–osmium isotope and platinum group element systematics of marine vs. non-marine organic-rich sediments and coals from Egypt. *Chemical Geology*, 285(1–4), 70–81. <https://doi.org/10.1016/j.chemgeo.2011.02.026>

Barra, F., Deditius, A., Reich, M., Kilburn, M. R., Guagliardo, P., & Roberts, M. P. (2017). Dissecting the Re-Os molybdenite geochronometer. *Scientific Reports*, 7(1), 16054. <https://doi.org/10.1038/s41598-017-16380-8>

Barton, I. F., Rathkopf, C. A., & Barton, M. D. (2020). Rhenium in molybdenite: A database approach to identifying geochemical controls on the distribution of a critical element. *Mining, Metallurgy & Exploration*, 37(1), 21–37. <https://doi.org/10.1007/s42461-019-00145-0>

Acknowledgments

LG acknowledges support from a GSA Graduate Student Research Grant. KEG was supported and partial writing of this work was performed under the auspices of the U.S. Department of Energy by Lawrence Livermore National Laboratory under Contract DE-AC52-07NA27344 and was supported by the LLNL LDRD Program under Project No. 24-LW-049 LLNL-JRNL-868303. AC was funded by NSF EAR Grants 2051199 and 2322206. MD received support from a postdoctoral fellowship from ISF-CNSF Grant (3413/21). BPE thanks Keiko Tagami for making data on Japanese rivers available in electronic format. JPR was funded by NSF EAR award 1655506.

Becker, H. (2000). Re–Os fractionation in eclogites and blueschists and the implications for recycling of oceanic crust into the mantle. *Earth and Planetary Science Letters*, 177(3), 287–300. [https://doi.org/10.1016/S0012-821X\(00\)00052-2](https://doi.org/10.1016/S0012-821X(00)00052-2)

Bennett, W. W., & Canfield, D. E. (2020). Redox-sensitive trace metals as paleoredox proxies: A review and analysis of data from modern sediments. *Earth-Science Reviews*, 204, 103175. <https://doi.org/10.1016/j.earscirev.2020.103175>

Bernard, A., Symonds, R. B., & Rose, W. I. (1990). Volatile transport and deposition of Mo, W and Re in high temperature magmatic fluids. *Applied Geochemistry*, 5(3), 317–326. [https://doi.org/10.1016/0883-2927\(90\)90007-R](https://doi.org/10.1016/0883-2927(90)90007-R)

Berner, E. K., & Berner, R. A. (2012). *Global environment: Water, air, and geochemical cycles*. Princeton University Press.

Berner, R. A. (2006). Geocarbsulf: A combined model for phanerozoic atmospheric O₂ and CO₂. *Geochimica et Cosmochimica Acta*, 70(23), 5653–5664. <https://doi.org/10.1016/j.gca.2005.11.032>

Bertine, K., & Goldberg, E. D. (1971). Fossil fuel combustion and the major sedimentary cycle. *Science*, 173(3993), 233–235. <https://doi.org/10.1126/science.173.3993.233>

Blusztajn, J., Hart, S., Ravizza, G., & Dick, H. (2000). Platinum-group elements and Os isotopic characteristics of the lower oceanic crust. *Chemical Geology*, 168(1–2), 113–122. [https://doi.org/10.1016/s0009-2541\(00\)00186-8](https://doi.org/10.1016/s0009-2541(00)00186-8)

Bluth, G., Schnetzler, C., Krueger, A., & Walter, L. (1993). The contribution of explosive volcanism to global atmospheric sulphur dioxide concentrations. *Nature*, 366(6453), 327–329. <https://doi.org/10.1038/366327a0>

Borisova, L., Ryabukhin, V., Bozhkov, O., & Tsvetkova, K. T. (2010). Field determination of rhenium in plants using catalytic test methods with dimethyldithiooxamide and Sulfonitrazo P. *Journal of Analytical Chemistry*, 65(5), 535–541. <https://doi.org/10.1134/s1061934810050163>

Bozhkov, O., Tsvetkova, C., & Blagoeva, T. (2007). Plant biosphere-natural extractor and concentrator of rhenium from soils and waters. Paper presented at the Proc. WSEAS Intl. Conf. on Waste Management, Water Polution, Air Pollution, Indoor Climate, Arcachon. France.

Brainard, J. L. (2023). The availability of primary rhenium as a by-product of copper and molybdenum mining. *Mineral Economics*, 1–17. <https://doi.org/10.1007/s13563-023-00392-0>

Brand, W. A., Coplen, T. B., Vogl, J., Rosner, M., & Prohaska, T. (2014). Assessment of international reference materials for isotope-ratio analysis (IUPAC Technical Report). *Pure and Applied Chemistry*, 86(3), 425–467. <https://doi.org/10.1515/pac-2013-1023>

Brenan, J. M. (2018). Rhenium. In W. M. White (Ed.), *Encyclopedia of geochemistry: A comprehensive reference source on the chemistry of the earth* (pp. 1312–1314).

Broadbent, H. S., Campbell, G. C., Bartley, W. J., & Johnson, J. H. (1959). Rhenium and its compounds as hydrogenation catalysts. III. Rhenium Heptoxide1, 2, 3. *Journal of Organic Chemistry*, 24(12), 1847–1854. <https://doi.org/10.1021/jo01094a003>

Brookins, D. G. (1986). Rhenium as analog for fissionogenic technetium: Eh-pH diagram (25°C, 1 bar) constraints. *Applied Geochemistry*, 1(4), 513–517. [https://doi.org/10.1016/0883-2927\(86\)90056-9](https://doi.org/10.1016/0883-2927(86)90056-9)

Brumsack, H.-J. (2006). The trace metal content of recent organic carbon-rich sediments: Implications for cretaceous black shale formation. *Palaeogeography, Palaeoclimatology, Palaeoecology*, 232(2–4), 344–361. <https://doi.org/10.1016/j.palaeo.2005.05.011>

Bura-Nakić, E., Knežević, L., Mandić, J., Cindrić, A.-M., & Omanović, D. (2021). Rhenium distribution and behavior in the salinity gradient of a highly stratified estuary and pristine riverine waters (the Krka River, Croatia). *Archives of Environmental Contamination and Toxicology*, 81(4), 564–573. <https://doi.org/10.1007/s00244-021-00876-6>

Burnett, W., Aggarwal, P., Aureli, A., Bokuniewicz, H., Cable, J., Charette, M., et al. (2006). Quantifying submarine groundwater discharge in the coastal zone via multiple methods. *Science of the Total Environment*, 367(2–3), 498–543. <https://doi.org/10.1016/j.scitotenv.2006.05.009>

Cakmur, R., Miller, R., Perlitz, J., Geogdzhayev, I., Ginoux, P., Koch, D., et al. (2006). Constraining the magnitude of the global dust cycle by minimizing the difference between a model and observations. *Journal of Geophysical Research*, 111(D06207). <https://doi.org/10.1029/2005jd005791>

Chappaz, A., Gobeil, C., & Tessier, A. (2008). Sequestration mechanisms and anthropogenic inputs of rhenium in sediments from Eastern Canada lakes. *Geochimica et Cosmochimica Acta*, 72(24), 6027–6036. <https://doi.org/10.1016/j.gca.2008.10.003>

Charette, M. A., & Sholkovitz, E. R. (2006). Trace element cycling in a subterranean estuary: Part 2. Geochemistry of the pore water. *Geochimica et Cosmochimica Acta*, 70(4), 811–826. <https://doi.org/10.1016/j.gca.2005.10.019>

Charette, M. A., & Smith, W. H. (2010). The volume of Earth's ocean. *Oceanography*, 23(2), 112–114. <https://doi.org/10.5670/oceanog.2010.51>

Cohen, A. S., Coe, A. L., Bartlett, J. M., & Hawkesworth, C. J. (1999). Precise Re–Os ages of organic-rich mudrocks and the Os isotope composition of Jurassic seawater. *Earth and Planetary Science Letters*, 167(3–4), 159–173. [https://doi.org/10.1016/s0012-821x\(99\)00026-6](https://doi.org/10.1016/s0012-821x(99)00026-6)

Colodner, D., Edmond, J., & Boyle, E. (1995). Rhenium in the Black Sea: Comparison with molybdenum and uranium. *Earth and Planetary Science Letters*, 131(1–2), 1–15. [https://doi.org/10.1016/0012-821x\(95\)00010-a](https://doi.org/10.1016/0012-821x(95)00010-a)

Colodner, D., Sachs, J., Ravizza, G., Turekian, K., Edmond, J., & Boyle, E. (1993). The geochemical cycle of rhenium: A reconnaissance. *Earth and Planetary Science Letters*, 117(1–2), 205–221. [https://doi.org/10.1016/0012-821x\(93\)90127-u](https://doi.org/10.1016/0012-821x(93)90127-u)

Corliss, J. B., Dymond, J., Gordon, L. I., Edmond, J. M., von Herzen, R. P., Ballard, R. D., et al. (1979). Submarine thermal springs on the Galapagos rift. *Science*, 203(4385), 1073–1083. <https://doi.org/10.1126/science.203.4385.1073>

Crusius, J., Calvert, S., Pedersen, T., & Sage, D. (1996). Rhenium and molybdenum enrichments in sediments as indicators of oxic, suboxic and sulfidic conditions of deposition. *Earth and Planetary Science Letters*, 145(1), 65–78. [https://doi.org/10.1016/S0012-821X\(96\)00204-X](https://doi.org/10.1016/S0012-821X(96)00204-X)

Crusius, J., & Thomson, J. (2000). Comparative behavior of authigenic Re, U, and Mo during reoxidation and subsequent long-term burial in marine sediments. *Geochimica et Cosmochimica Acta*, 64(13), 2233–2242. [https://doi.org/10.1016/s0016-7037\(99\)00433-0](https://doi.org/10.1016/s0016-7037(99)00433-0)

Dai, S., Finkelman, R. B., French, D., Hower, J. C., Graham, I. T., & Zhao, F. (2021). Modes of occurrence of elements in coal: A critical evaluation. *Earth-Science Reviews*, 222, 103815. <https://doi.org/10.1016/j.earscirev.2021.103815>

Dai, S., Seredin, V. V., Ward, C. R., Hower, J. C., Xing, Y., Zhang, W., et al. (2015). Enrichment of U–Se–Mo–Re–V in coals preserved within marine carbonate successions: Geochemical and mineralogical data from the late Permian guiding coalfield, Guizhou, China. *Mineralium Deposita*, 50(2), 159–186. <https://doi.org/10.1007/s00126-014-0528-1>

Dalai, T. K., Singh, S. K., Trivedi, J., & Krishnaswami, S. (2002). Dissolved rhenium in the Yamuna River System and the Ganga in the Himalaya: Role of black shale weathering on the budgets of Re, Os, and U in rivers and CO₂ in the atmosphere. *Geochimica et Cosmochimica Acta*, 66(1), 29–43. [https://doi.org/10.1016/s0016-7037\(01\)00747-5](https://doi.org/10.1016/s0016-7037(01)00747-5)

Dale, C. W., Gannoun, A., Burton, K. W., Argles, T. W., & Parkinson, I. J. (2007). Rhenium–osmium isotope and elemental behaviour during subduction of oceanic crust and the implications for mantle recycling. *Earth and Planetary Science Letters*, 253(1), 211–225. <https://doi.org/10.1016/j.epsl.2006.10.029>

Danish, M., Tripathy, G. R., Mitra, S., Rout, R. K., & Raskar, S. (2021). Non-conservative removal of dissolved rhenium from a coastal lagoon: Clay adsorption versus biological uptake. *Chemical Geology*, 580, 120378. <https://doi.org/10.1016/j.chemgeo.2021.120378>

Dellingier, M., Hilton, R. G., & Nowell, G. M. (2020). Measurements of rhenium isotopic composition in low-abundance samples. *Journal of Analytical Atomic Spectrometry*, 35(2), 377–387. <https://doi.org/10.1039/c9ja00288j>

Dellinger, M., Hilton, R. G., & Nowell, G. M. (2021). Fractionation of rhenium isotopes in the Mackenzie River basin during oxidative weathering. *Earth and Planetary Science Letters*, 573, 117131. <https://doi.org/10.1016/j.epsl.2021.117131>

Dellinger, M., Hilton, R. G., Torres, M. A., Burt, E. I., Baronas, J. J., Clark, K. E., et al. (2023). High rates of rock organic carbon oxidation sustained as Andean sediment transits the Amazon foreland-floodplain. *Proceedings of the National Academy of Sciences*, 120(39), e2306343120. <https://doi.org/10.1073/pnas.2306343120>

Dellwig, O., Böttcher, M. E., Lipinski, M., & Brumsack, H.-J. (2002). Trace metals in Holocene coastal peats and their relation to pyrite formation (NW Germany). *Chemical Geology*, 182(2–4), 423–442. [https://doi.org/10.1016/s0009-2541\(01\)00335-7](https://doi.org/10.1016/s0009-2541(01)00335-7)

Dickson, A. J., Hsieh, Y.-T., & Bryan, A. (2020). The rhenium isotope composition of Atlantic Ocean seawater. *Geochimica et Cosmochimica Acta*, 287, 221–228. <https://doi.org/10.1016/j.gca.2020.02.020>

Dolor, M. K., Gilmour, C. C., & Helz, G. R. (2009). Distinct microbial behavior of Re compared to Tc: Evidence against microbial Re fixation in aquatic sediments. *Geomicrobiology Journal*, 26(7), 470–483. <https://doi.org/10.1080/01490450903060822>

Ermakov, V., Safonov, V., & Dogadkin, D. (2021). Characteristic features of molybdenum, copper, tungsten and rhenium accumulation in the environment. *Innovative Infrastructure Solutions*, 6(2), 1–7. <https://doi.org/10.1007/s41062-021-00481-5>

Esser, B. K., & Turekian, K. K. (1993). The osmium isotopic composition of the continental crust. *Geochimica et Cosmochimica Acta*, 57(13), 3093–3104. [https://doi.org/10.1016/0016-7037\(93\)90296-9](https://doi.org/10.1016/0016-7037(93)90296-9)

Fritsche, J., & Meisel, T. (2004). Determination of anthropogenic input of Ru, Rh, Pd, Re, Os, Ir and Pt in soils along Austrian motorways by isotope dilution ICP-MS. *Science of the Total Environment*, 325(1–3), 145–154. <https://doi.org/10.1016/j.scitotenv.2003.11.019>

Gaillardet, J., Dupré, B., & Allègre, C. J. (1995). A global geochemical mass budget applied to the Congo Basin Rivers: Erosion rates and continental crust composition. *Geochimica et Cosmochimica Acta*, 59(17), 3469–3485. [https://doi.org/10.1016/0016-7037\(95\)00230-w](https://doi.org/10.1016/0016-7037(95)00230-w)

Gaillardet, J., Viers, J., & Dupré, B. (2003). Trace elements in river waters. In H. Holland & K. Turekian (Eds.), *Treatise on geochemistry* (2nd ed., Vol. 5, pp. 225–272). Elsevier.

Geiss, J., Hirt, B., Signer, P., Herr, W., & Merz, E. (1958). Isotope analysis of osmium in the Henbury meteorite. *Helvetica Physica Acta*, 31, 324–325.

Ghazi, L., Goñi, M., Haley, B. A., Muratli, J. M., & Pett-Ridge, J. C. (2022). Concentration-runoff relationships of contrasting small mountainous rivers in the Pacific Northwest, USA: Insights into the weathering of rhenium relative to other weathering products. *Geochimica et Cosmochimica Acta*, 337, 106–122. <https://doi.org/10.1016/j.gca.2022.09.036>

Ghazi, L., Grant, K., Chappaz, A., Danish, M., Peucker-Ehrenbrink, B., & Pett-Ridge, J. (2024). The global biogeochemical cycle of rhenium [Dataset]. *Global Biogeochemical Cycles*. Zenodo. <https://doi.org/10.5281/zenodo.11624420>

Goswami, V., Hannah, J. L., & Stein, H. J. (2018). Why terrestrial coals cannot be dated using the Re-Os geochronometer: Evidence from the Finnmark platform, southern Barents Sea and the fire clay coal horizon, central Appalachian basin. *International Journal of Coal Geology*, 188, 121–135. <https://doi.org/10.1016/j.coal.2018.02.005>

Graham, S., Famiglietti, J., & Maidment, D. (1999). Five-minute, 1/2°, and 1° data sets of continental watersheds and river networks for use in regional and global hydrologic and climate system modeling studies. *Water Resources Research*, 35(2), 583–587. <https://doi.org/10.1029/1998wr900068>

Gramlich, J. W., Murphy, T. J., Garner, E. L., & Shields, W. R. (1973). Absolute isotopic abundance ratio and atomic weight of a reference sample of rhenium. *Journal of Research of the National Bureau of Standards. Section A, Physics and Chemistry*, 77A(6), 691–698. <https://doi.org/10.6028/jres.077a.040>

Gu, X., Heaney, P. J., Reis, F. D. A. A., & Brantley, S. L. (2020). Deep abiotic weathering of pyrite. *Science*, 370(6515), eabb8092. <https://doi.org/10.1126/science.abb8092>

Hartmann, J., & Moosdorf, N. (2012). The new global lithological map database GLiM: A representation of rock properties at the earth surface. *Geochemistry, Geophysics, Geosystems*, 13(12), Q12004. <https://doi.org/10.1029/2012GC004370>

He, H., Dong, Z., Pang, J., Wu, G.-L., Zheng, J., & Zhang, X. (2018). Phytoextraction of rhenium by lucerne (*Medicago sativa*) and erect milkvetch (*Astragalus adsurgens*) from alkaline soils amended with coal fly ash. *Science of the Total Environment*, 630, 570–577. <https://doi.org/10.1016/j.scitotenv.2018.02.252>

Helz, G. R. (2022). The Re/Mo redox proxy reconsidered. *Geochimica et Cosmochimica Acta*, 317, 507–522. <https://doi.org/10.1016/j.gca.2021.10.029>

Helz, G. R., & Adelson, J. M. (2013). Trace element profiles in sediments as proxies of dead zone history: rhenium compared to molybdenum. *Environmental Science & Technology*, 47(3), 1257–1264. <https://doi.org/10.1021/es303138d>

Helz, G. R., & Dolor, M. K. (2012). What regulates rhenium deposition in euxinic basins? *Chemical Geology*, 304–305, 131–141. <https://doi.org/10.1016/j.chemgeo.2012.02.011>

Herr, W., Hintenberger, H., & Voshage, H. (1954). Half-life of rhenium. *Physical Review*, 95(6), 1691. <https://doi.org/10.1103/physrev.95.1691>

Herr, W., Hoffmeister, W., Langhoff, J., Geiss, J., Hirt, B., & Houtermans, F. (1962). Os 187-isotope abundances in terrestrial and meteoritic osmium and an attempt to determine Re/Os-ages of iron meteorites. Paper presented at the Radioisotopes in the Physical Sciences and Industry. Proceedings of the Conference on the Use of Radioisotopes in the Physical Sciences and Industry. V. 1.

Hilton, R. G., Gaillardet, J., Calmels, D., & Birek, J.-L. (2014). Geological respiration of a mountain belt revealed by the trace element rhenium. *Earth and Planetary Science Letters*, 403, 27–36. <https://doi.org/10.1016/j.epsl.2014.06.021>

Hilton, R. G., Turowski, J. M., Winnick, M., Dellinger, M., Schleppi, P., Williams, K. H., et al. (2021). Concentration-discharge relationships of dissolved rhenium in alpine catchments reveal its use as a tracer of oxidative weathering. *Water Resources Research*, 57(11), e2021WR029844. <https://doi.org/10.1029/2021WR029844>

Hilton, R. G., & West, A. J. (2020). Mountains, erosion and the carbon cycle. *Nature Reviews Earth & Environment*, 1(6), 284–299. <https://doi.org/10.1038/s43017-020-0058-6>

Hinkley, T. K., Lamothe, P. J., Wilson, S. A., Finnegan, D. L., & Gerlach, T. M. (1999). Metal emissions from Kilauea, and a suggested revision of the estimated worldwide metal output by quiescent degassing of volcanoes. *Earth and Planetary Science Letters*, 170(3), 315–325. [https://doi.org/10.1016/s0012-821x\(99\)00103-x](https://doi.org/10.1016/s0012-821x(99)00103-x)

Hintenberger, H., Herr, W., & Voshage, H. (1954). Radiogenic osmium from rhenium-containing molybdenite. *Physical Review*, 95(6), 1690–1691. <https://doi.org/10.1103/physrev.95.1690>

Hisamatsu, Y., Egashira, K., & Maeno, Y. (2022). Ogawa's nipponium and its re-assignment to rhenium. *Foundations of Chemistry*, 24(1), 15–57. <https://doi.org/10.1007/s10698-021-09410-x>

Hlohowskyj, S. R., Chappaz, A., & Dickson, A. J. (2021). *Molybdenum as a paleoredox proxy: Past, present, and future*. Cambridge University Press.

Ho, P., Shim, M. J., Howden, S. D., & Shiller, A. M. (2019). Temporal and spatial distributions of nutrients and trace elements (Ba, Cs, Cr, Fe, Mn, Mo, U, V and Re) in Mississippi coastal waters: Influence of hypoxia, submarine groundwater discharge, and episodic events. *Continental Shelf Research*, 175, 53–69. <https://doi.org/10.1016/j.csr.2019.01.013>

Hodge, V. F., Johannesson, K. H., & Stetzenbach, K. J. (1996). Rhenium, molybdenum, and uranium in groundwater from the southern great basin, USA: Evidence for conservative behavior. *Geochimica et Cosmochimica Acta*, 60(17), 3197–3214. [https://doi.org/10.1016/0016-7037\(96\)00183-4](https://doi.org/10.1016/0016-7037(96)00183-4)

Hong, Q., Cheng, Y., Qu, Y., Wei, L., Liu, Y., Gao, J., et al. (2024). Overlooked shelf sediment reductive sinks of dissolved rhenium and uranium in the modern ocean. *Nature Communications*, 15(1), 3966. <https://doi.org/10.1038/s41467-024-48297-y>

Horan, K., Hilton, R. G., Dellingar, M., Tipper, E., Galy, V., Calmels, D., et al. (2019). Carbon dioxide emissions by rock organic carbon oxidation and the net geochemical carbon budget of the Mackenzie River Basin. *American Journal of Science*, 319(6), 473–499. <https://doi.org/10.2475/06.2019.02>

Horan, K., Hilton, R. G., Selby, D., Ottley, C. J., Gröcke, D. R., Hicks, M., & Burton, K. W. (2017). Mountain glaciation drives rapid oxidation of rock-bound organic carbon. *Science Advances*, 3(10), e1701107. <https://doi.org/10.1126/sciadv.1701107>

IEA. (2022). Coal 2022. Retrieved from Paris <https://www.iea.org/reports/coal-2022>

Ishida, M., Nozaki, T., Takaya, Y., Ohta, J., Chang, Q., Kimura, J.-I., et al. (2022). Re–Os geochemistry of hydrothermally altered dacitic rock in a submarine volcano at Site U1527, IODP Expedition 376: Implications for the Re cycle in intraoceanic arcs. *Deep Sea Research Part I: Oceanographic Research Papers*, 180, 103687. <https://doi.org/10.1016/j.dsr.2021.103687>

Jaffe, L. A., Peucker-Ehrenbrink, B., & Petsch, S. T. (2002). Mobility of rhenium, platinum group elements and organic carbon during black shale weathering. *Earth and Planetary Science Letters*, 198(3–4), 339–353. [https://doi.org/10.1016/s0012-821x\(02\)00526-5](https://doi.org/10.1016/s0012-821x(02)00526-5)

John, D., Seal II, R. R., & Polyak, D. E. (2017). Rhenium. In K. J. Schulz, J. J. H. DeYoung, R. R. Seal II, & D. C. Bradley (Eds.), *Critical mineral resources of the United States—Economic and environmental geology and prospects for future supply* (p. 62). Survey, U. S. G. (Series Ed.). <https://doi.org/10.3133/pp1802>

Kablov, E., Petrushin, N., Bronfin, M., & Alekseev, A. (2006). Specific features of rhenium-alloyed single-crystal nickel superalloys. *Russian Metallurgy*, 2006(5), 406–414. <https://doi.org/10.1134/s0036029506050089>

Kendall, B. S., Creaser, R. A., Ross, G. M., & Selby, D. (2004). Constraints on the timing of Marinoan “Snowball Earth” glaciation by ^{187}Re – ^{187}Os dating of a Neoproterozoic, post-glacial black shale in Western Canada. *Earth and Planetary Science Letters*, 222(3–4), 729–740. <https://doi.org/10.1016/j.epsl.2004.04.004>

Kidder, J., McClenaghan, M., Leybourne, M., McCurdy, M., Pelchat, P., Layton-Matthews, D., & Voinot, A. (2022). Hydrogeochemistry of porphyry-related solutes in ground and surface waters: an example from the Casino Cu–Au–Mo deposit, Yukon, Canada. *Geochemistry: Exploration, Environment, Analysis*, 22(2), geochem2021-2058. <https://doi.org/10.1144/geochem2021-058>

Kilber, A. W., Boyanov, M. I., Kemner, K. M., & O’Loughlin, E. J. (2024). Interactions of perrhenate ($\text{Re}(\text{VII})\text{O}_4^-$) with Fe (II)-bearing minerals. *Minerals*, 14(2), 181. <https://doi.org/10.3390/min14020181>

Killingsworth, B. A., & Bao, H. (2015). Significant human impact on the flux and $\delta^{34}\text{S}$ of sulfate from the Largest River in North America. *Environmental Science & Technology*, 49(8), 4851–4860. <https://doi.org/10.1021/es504498s>

Kim, E., Benedetti, M. F., & Boulègue, J. (2004). Removal of dissolved rhenium by sorption onto organic polymers: Study of rhenium as an analogue of radioactive technetium. *Water Research*, 38(2), 448–454. <https://doi.org/10.1016/j.watres.2003.09.033>

Klee, R., & Graedel, T. (2004). Elemental cycles: A status report on human or natural dominance. *Annual Review of Environment and Resources*, 29(1), 69–107. <https://doi.org/10.1146/annurev.energy.29.042203.104034>

Koide, M., Hodge, V., Yang, J., Stallard, M., Goldberg, E., Calhoun, J., & Bertine, K. (1986). Some comparative marine chemistries of rhenium, gold, silver and molybdenum. *Applied Geochemistry*, 1(6), 705–714. [https://doi.org/10.1016/0883-2927\(86\)90092-2](https://doi.org/10.1016/0883-2927(86)90092-2)

Krähenbühl, U., Geissbühler, M., Bühl, F., Eberhardt, P., & Finnegan, D. L. (1992). Osmium isotopes in the aerosols of the mantle volcano Mauna Loa. *Earth and Planetary Science Letters*, 110(1–4), 95–98. [https://doi.org/10.1016/0012-821x\(92\)90041-s](https://doi.org/10.1016/0012-821x(92)90041-s)

Kučera, J., Kučera, J., Byrne, A., Byrne, A., Mizera, J., Mizera, J., et al. (2006). Development of a radiochemical neutron activation analysis procedure for determination of rhenium in biological and environmental samples at ultratrace level. *Journal of Radioanalytical and Nuclear Chemistry*, 269(2), 251–257. <https://doi.org/10.1007/s10967-006-0331-2>

La Flèche, M., Cuss, C. W., Noernberg, T., Shotyk, W., & Karst, J. (2021). Trace metals as indicators of tree rooting in bituminous soils. *Land Degradation & Development*, 32(5), 1970–1980. <https://doi.org/10.1002/lrd.3848>

Laing, J. R., Hopke, P. K., Hopke, E. F., Husain, L., Dutkiewicz, V. A., Paatero, J., & Viiisanen, Y. (2014a). Long-term particle measurements in Finnish Arctic: Part I–Chemical composition and trace metal solubility. *Atmospheric Environment*, 88, 275–284. <https://doi.org/10.1016/j.atmosenv.2014.03.002>

Laing, J. R., Hopke, P. K., Hopke, E. F., Husain, L., Dutkiewicz, V. A., Paatero, J., & Viiisanen, Y. (2014b). Long-term particle measurements in Finnish Arctic: Part II–Trend analysis and source location identification. *Atmospheric Environment*, 88, 285–296. <https://doi.org/10.1016/j.atmosenv.2014.01.015>

Lassiter, J. C. (2003). Rhenium volatility in subaerial lavas: Constraints from subaerial and submarine portions of the HSDP-2 Mauna Kea drillcore. *Earth and Planetary Science Letters*, 214(1–2), 311–325. [https://doi.org/10.1016/s0012-821x\(03\)00385-6](https://doi.org/10.1016/s0012-821x(03)00385-6)

Leybourne, M. I., & Cameron, E. M. (2008). Source, transport, and fate of rhenium, selenium, molybdenum, arsenic, and copper in groundwater associated with porphyry–Cu deposits, Atacama Desert, Chile. *Chemical Geology*, 247(1–2), 208–228. <https://doi.org/10.1016/j.chemgeo.2007.10.017>

Liu, R., Hu, L., & Humayun, M. (2017). Natural variations in the rhenium isotopic composition of meteorites. *Meteoritics & Planetary Sciences*, 52(3), 479–492. <https://doi.org/10.1111/maps.12803>

Love, S., & Brownlee, D. (1993). A direct measurement of the terrestrial mass accretion rate of cosmic dust. *Science*, 262(5133), 550–553. <https://doi.org/10.1126/science.262.5133.550>

Luck, J.-M., Birck, J.-L., & Allegre, C.-J. (1980). ^{187}Re – ^{187}Os systematics in meteorites: Early chronology of the solar system and age of the Galaxy. *Nature*, 283(5744), 256–259. <https://doi.org/10.1038/283256a0>

Lyons, T. W., Diamond, C. W., Planavsky, N. J., Reinhard, C. T., & Li, C. (2021). Oxygenation, life, and the planetary system during Earth’s middle history: An overview. *Astrobiology*, 21(8), 906–923. <https://doi.org/10.1089/ast.2020.2418>

Mas, J., Tagami, K., & Uchida, S. (2005). Rhenium measurements on North Atlantic seaweed samples by ID-ICP-MS: An observation on the Re concentration factors. *Journal of Radioanalytical and Nuclear Chemistry*, 265(3), 361–365. <https://doi.org/10.1007/s10967-005-0833-3>

Mather, T., Witt, M., Pyle, D., Quayle, B., Aiuppa, A., Bagnato, E., et al. (2012). Halogens and trace metal emissions from the ongoing 2008 summit eruption of Kilauea volcano, Hawaii. *Geochimica et Cosmochimica Acta*, 83, 292–323. <https://doi.org/10.1016/j.gca.2011.11.029>

Maun, E. K., & Davidson, N. (1950). Investigations in the chemistry of rhenium. I. Oxidation states IV, V and VII, 2. *Journal of the American Chemical Society*, 72(5), 2254–2260. <https://doi.org/10.1021/ja01161a104>

Mayfield, K. K., Eisenhauer, A., Santiago Ramos, D. P., Higgins, J. A., Horner, T. J., Auro, M., et al. (2021). Groundwater discharge impacts marine isotope budgets of Li, Mg, Ca, Sr, and Ba. *Nature Communications*, 12(1), 148. <https://doi.org/10.1038/s41467-020-20248-3>

McLennan, S. M. (2001). Relationships between the trace element composition of sedimentary rocks and upper continental crust. *Geochemistry, Geophysics, Geosystems*, 2(4), Q000109. <https://doi.org/10.1029/2000GC000109>

Melián, C., Kremer, C., Suescun, L., Mombrú, A., Mariezcurrena, R., & Kremer, E. (2000). Re(V) complexes with amino acids based on the '3+2' approach. *Inorganica Chimica Acta*, 306(1), 70–77. [https://doi.org/10.1016/s0020-1693\(00\)00151-1](https://doi.org/10.1016/s0020-1693(00)00151-1)

Meybeck, M. (1979). Concentrations des eaux fluviales en éléments majeurs et apports en solution aux océans. *Revue de Géologie Dynamique et de Géographie Physique*, 21, 215–246.

Meybeck, M. (1988). How to establish and use world budgets of riverine materials. In A. Lerman & M. Meybeck (Eds.), *Physical and chemical weathering in geochemical cycles* (Vol. 251, pp. 247–272). Springer. https://doi.org/10.1007/978-94-009-3071-1_12

Meybeck, M., & Helmer, R. (1989). The quality of rivers: From pristine stage to global pollution. *Palaeogeography, Palaeoclimatology, Palaeoecology*, 75(4), 283–309. [https://doi.org/10.1016/0031-0182\(89\)90191-0](https://doi.org/10.1016/0031-0182(89)90191-0)

Meybeck, M., & Ragu, A. (2012). *GEMS-GLORI world river discharge database*. Laboratoire de Géologie Appliquée. Université Pierre et Marie Curie.

Miller, C. A. (2004). Re-Os dating of algal laminites: Reduction-enrichment of metals in the sedimentary environment and evidence for new geoporphyrins. (M.Sc.). University of Saskatchewan.

Miller, C. A. (2009). *Surface-cycling of rhenium and its isotopes* (Ph.D. Thesis). MIT/WHOI.

Miller, C. A., Peucker-Ehrenbrink, B., & Ball, L. (2009). Precise determination of rhenium isotope composition by multi-collector inductively-coupled plasma mass spectrometry. *Journal of Analytical Atomic Spectrometry*, 24(8), 1069–1078. <https://doi.org/10.1039/b818631f>

Miller, C. A., Peucker-Ehrenbrink, B., & Schauble, E. A. (2015). Theoretical modeling of rhenium isotope fractionation, natural variations across a black shale weathering profile, and potential as a paleoredox proxy. *Earth and Planetary Science Letters*, 430, 339–348. <https://doi.org/10.1016/j.epsl.2015.08.008>

Miller, C. A., Peucker-Ehrenbrink, B., Walker, B. D., & Marcantonio, F. (2011). Re-assessing the surface cycling of molybdenum and rhenium. *Geochimica et Cosmochimica Acta*, 75(22), 7146–7179. <https://doi.org/10.1016/j.gca.2011.09.005>

Moiseenko, T., Gashkina, N., & Dinu, M. (2016). Enrichment of surface water by elements: Effects of air pollution, acidification and eutrophication. *Environmental Processes*, 3(1), 39–58. <https://doi.org/10.1007/s40710-016-0132-8>

Moore, W. S. (1997). High fluxes of radium and barium from the mouth of the Ganges-Brahmaputra River during low river discharge suggest a large groundwater source. *Earth and Planetary Science Letters*, 150(1–2), 141–150. [https://doi.org/10.1016/s0012-821x\(97\)00083-6](https://doi.org/10.1016/s0012-821x(97)00083-6)

Morel, J.-L., Echevarria, G., & Goncharova, N. (2006). *Phytoremediation of metal-contaminated soils* (Vol. 68). Springer Science & Business Media.

Morford, J. L., Emerson, S. R., Breckel, E. J., & Kim, S. H. (2005). Diagenesis of oxyanions (V, U, Re, and Mo) in pore waters and sediments from a continental margin. *Geochimica et Cosmochimica Acta*, 69(21), 5021–5032. <https://doi.org/10.1016/j.gca.2005.05.015>

Morford, J. L., Martin, W. R., & Carney, C. M. (2012). Rhenium geochemical cycling: Insights from continental margins. *Chemical Geology*, 324, 73–86. <https://doi.org/10.1016/j.chemgeo.2011.12.014>

Morford, J. L., Martin, W. R., François, R., & Carney, C. M. (2009). A model for uranium, rhenium, and molybdenum diagenesis in marine sediments based on results from coastal locations. *Geochimica et Cosmochimica Acta*, 73(10), 2938–2960. <https://doi.org/10.1016/j.gca.2009.02.029>

Morford, J. L., Martin, W. R., Kalnejais, L. H., François, R., Bothner, M., & Karle, I.-M. (2007). Insights on geochemical cycling of U, Re and Mo from seasonal sampling in Boston Harbor, Massachusetts, USA. *Geochimica et Cosmochimica Acta*, 71(4), 895–917. <https://doi.org/10.1016/j.gca.2006.10.016>

Mottl, M. J., & Wheat, C. G. (1994). Hydrothermal circulation through mid-ocean ridge flanks: Fluxes of heat and magnesium. *Geochimica et Cosmochimica Acta*, 58(10), 2225–2237. [https://doi.org/10.1016/0016-7037\(94\)90007-8](https://doi.org/10.1016/0016-7037(94)90007-8)

Mulligan, A. E., & Charette, M. A. (2006). Intercomparison of submarine groundwater discharge estimates from a sandy unconfined aquifer. *Journal of Hydrology*, 327(3–4), 411–425. <https://doi.org/10.1016/j.jhydrol.2005.11.056>

Naldrett, S., & Libby, W. (1948). Natural radioactivity of rhenium. *Physical Review*, 73(5), 487–496. <https://doi.org/10.1103/PhysRev.73.487>

Nameroff, T., Balistrieri, L., & Murray, J. (2002). Suboxic trace metal geochemistry in the eastern tropical North Pacific. *Geochimica et Cosmochimica Acta*, 66(7), 1139–1158. [https://doi.org/10.1016/s0016-7037\(01\)00843-2](https://doi.org/10.1016/s0016-7037(01)00843-2)

Naumov, A. V. (2007). Rhythms of rhenium. *Russian Journal of Non-Ferrous Metals*, 48(6), 418–423. <https://doi.org/10.3103/S1067821207060089>

Nikolaychuk, P. A. (2022). The potential–pH diagram for rhenium. *Chemical Thermodynamics and Thermal Analysis*, 7, 100068. <https://doi.org/10.1016/j.ctta.2022.100068>

Noddack, I., & Noddack, W. (1927). Darstellung und einige chemische Eigenschaften des Rheniums. *Zeitschrift für Physikalische Chemie*, 125(1), 264–274. <https://doi.org/10.1515/zpch-1927-12516>

Noddack, I., Noddack, W., & Berg, O. (1925). Die Ekamangane. *Naturwissenschaften*, 13(26), 567–574. <https://doi.org/10.1007/BF01558746>

Novo, L. A., Silva, E. F., Pereira, A., Casanova, A., & González, L. (2018). The effects of rhenium accumulation on Indian mustard. *Environmental Science and Pollution Research*, 25(21), 21243–21250. <https://doi.org/10.1007/s11356-018-2547-4>

Ogawa, M. (1908a). Preliminary note on a new element allied to molybdenum. *Chemical News*, 28, 261–264.

Ogawa, M. (1908b). Preliminary note on a new element in thorianite. *Journal of the College of Science. Imperial University of Tokyo*, Japan, 25.

Ogric, M., Dellingen, M., Grant, K. E., Galy, V., Gu, X., Brantley, S. L., & Hilton, R. G. (2023). Low rates of rock organic carbon oxidation and anthropogenic cycling of rhenium in a slowly denuding landscape. *Earth Surface Processes and Landforms*, 48(6), 1202–1218. <https://doi.org/10.1002/esp.5543>

Peretyazhko, T., Zachara, J. M., Heald, S. M., Jeon, B.-H., Kukkadapu, R. K., Liu, C., et al. (2008). Heterogeneous reduction of Tc (VII) by Fe (II) at the solid–water interface. *Geochimica et Cosmochimica Acta*, 72(6), 1521–1539. <https://doi.org/10.1016/j.gca.2008.01.004>

Peretyazhko, T., Zachara, J. M., Kukkadapu, R. K., Heald, S. M., Kutnyakov, I. V., Resch, C. T., et al. (2012). Pertechnetate (TcO₄[–]) reduction by reactive ferrous iron forms in naturally anoxic, redox transition zone sediments from the Hanford Site, USA. *Geochimica et Cosmochimica Acta*, 92, 48–66. <https://doi.org/10.1016/j.gca.2012.05.041>

Petsch, S., Berner, R., & Eglington, T. (2000). A field study of the chemical weathering of ancient sedimentary organic matter. *Organic Geochemistry*, 31(5), 475–487. [https://doi.org/10.1016/s0146-6380\(00\)00014-0](https://doi.org/10.1016/s0146-6380(00)00014-0)

Peucker-Ehrenbrink, B. (2018). *Land2Sea database*, version 2.0. Pangaea.

Peucker-Ehrenbrink, B., Bach, W., Hart, S. R., Bluszta, J. S., & Abbruzzese, T. (2003). Rhenium–osmium isotope systematics and platinum group element concentrations in oceanic crust from DSDP/ODP Sites 504 and 417/418. *Geochemistry, Geophysics, Geosystems*, 4(7), 2002GC000414. <https://doi.org/10.1029/2002gc000414>

Peucker-Ehrenbrink, B., & Hannigan, R. E. (2000). Effects of black shale weathering on the mobility of rhenium and platinum group elements. *Geology*, 28(5), 475–478. [https://doi.org/10.1130/0091-7613\(2000\)28<475:eboswo>2.0.co;2](https://doi.org/10.1130/0091-7613(2000)28<475:eboswo>2.0.co;2)

Peucker-Ehrenbrink, B., & Jahn, B. m. (2001). Rhenium-osmium isotope systematics and platinum group element concentrations: Loess and the upper continental crust. *Geochemistry, Geophysics, Geosystems*, 2(10), Q000172. <https://doi.org/10.1029/2001gc000172>

Peucker-Ehrenbrink, B., & Ravizza, G. (2000). The effects of sampling artifacts on cosmic dust flux estimates: A reevaluation of nonvolatile tracers (Os, Ir). *Geochimica et Cosmochimica Acta*, 64(11), 1965–1970. [https://doi.org/10.1016/s0016-7037\(99\)00429-9](https://doi.org/10.1016/s0016-7037(99)00429-9)

Pierson-Wickmann, A.-C., Reisberg, L., & France-Lanord, C. (2002). Behavior of Re and Os during low-temperature alteration: Results from Himalayan soils and altered black shales. *Geochimica et Cosmochimica Acta*, 66(9), 1539–1548. [https://doi.org/10.1016/s0016-7037\(01\)00865-1](https://doi.org/10.1016/s0016-7037(01)00865-1)

Poirier, A., & Hillaire-Marcel, C. (2011). Improved Os-isotope stratigraphy of the Arctic Ocean. *Geophysical Research Letters*, 38(14), L14607. <https://doi.org/10.1029/2011gl047953>

Polyak, D. E. (2021). Rhenium [2021 tables-only release]. Retrieved from <https://www.usgs.gov/centers/national-minerals-information-center/rhenium-statistics-and-information>

Prouty, N. G., Roark, E. B., Koenig, A. E., Demopoulos, A. W., Batista, F. C., Kocar, B. D., et al. (2014). Deep-sea coral record of human impact on watershed quality in the Mississippi River Basin. *Global Biogeochemical Cycles*, 28(1), 29–43. <https://doi.org/10.1002/2013gb004754>

Racionero-Gómez, B., Sproson, A. D., Selby, D., Gröcke, D. R., Redden, H., & Greenwell, H. C. (2016). Rhenium uptake and distribution in phaeophyceae macroalgae, *Fucus vesiculosus*. *Royal Society Open Science*, 3(5), 160161. <https://doi.org/10.1098/rsos.160161>

Rahaman, W., & Singh, S. K. (2010). Rhenium in rivers and estuaries of India: Sources, transport and behaviour. *Marine Chemistry*, 118(1–2), 1–10. <https://doi.org/10.1016/j.marchem.2009.09.008>

Rahaman, W., Singh, S. K., & Shukla, A. D. (2012). Rhenium in Indian rivers: Sources, fluxes, and contribution to oceanic budget. *Geochemistry, Geophysics, Geosystems*, 13(8), Q08019. <https://doi.org/10.1029/2012gc004083>

Ravizza, G., Martin, C., German, C., & Thompson, G. (1996). Os isotopes as tracers in seafloor hydrothermal systems: Metalliferous deposits from the TAG hydrothermal area, 26 N mid-Atlantic Ridge. *Earth and Planetary Science Letters*, 138(1–4), 105–119. [https://doi.org/10.1016/0012-821x\(95\)00216-y](https://doi.org/10.1016/0012-821x(95)00216-y)

Ravizza, G., & Turekian, K. K. (1989). Application of the ^{187}Re - ^{187}Os system to black shale geochronometry. *Geochimica et Cosmochimica Acta*, 53(12), 3257–3262. [https://doi.org/10.1016/0016-7037\(89\)90105-1](https://doi.org/10.1016/0016-7037(89)90105-1)

Ravizza, G., Turekian, K. K., & Hay, B. J. (1991). The geochemistry of rhenium and osmium in recent sediments from the Black Sea. *Geochimica et Cosmochimica Acta*, 55(12), 3741–3752. [https://doi.org/10.1016/0016-7037\(91\)90072-d](https://doi.org/10.1016/0016-7037(91)90072-d)

Reckhardt, A., Beck, M., Greskowiak, J., Schnetger, B., Böttcher, M. E., Gehre, M., & Brumsack, H.-J. (2017). Cycling of redox-sensitive elements in a sandy subterranean estuary of the southern North Sea. *Marine Chemistry*, 188, 6–17. <https://doi.org/10.1016/j.marchem.2016.11.003>

Reisberg, L., Rouxel, O., Ludden, J., Staudigel, H., & Zimmermann, C. (2008). Re–Os results from ODP Site 801: Evidence for extensive Re uptake during alteration of oceanic crust. *Chemical Geology*, 248(3–4), 256–271. <https://doi.org/10.1016/j.chemgeo.2007.07.013>

Righter, K., Chesley, J., Geist, D., & Ruiz, J. (1998). Behavior of Re during magma fractionation: An example from volcano Alcedo, Galapagos. *Journal of Petrology*, 39(4), 785–795. <https://doi.org/10.1093/petroj/39.4.785>

Riley, G. H. (1967). Rhenium concentration in Australian molybdenites by stable isotope dilution. *Geochimica et Cosmochimica Acta*, 31(9), 1489–1497. [https://doi.org/10.1016/0016-7037\(67\)90024-5](https://doi.org/10.1016/0016-7037(67)90024-5)

Riley, G. H., & Delong, S. E. (1970). Osmium isotopes in geology. *International Journal of Mass Spectrometry and Ion Physics*, 4(4), 297–304. [https://doi.org/10.1016/0020-7381\(70\)80545-8](https://doi.org/10.1016/0020-7381(70)80545-8)

Rodushkin, I., Engström, E., Sörlin, D., Pontér, C., & Baxter, D. C. (2007). Osmium in environmental samples from Northeast Sweden: Part I. Evaluation of background status. *Science of the Total Environment*, 386(1–3), 145–158. <https://doi.org/10.1016/j.scitotenv.2007.06.011>

Rooney, A. D., Selby, D., Lewan, M. D., Lillis, P. G., & Houzay, J.-P. (2012). Evaluating Re–Os systematics in organic-rich sedimentary rocks in response to petroleum generation using hydrous pyrolysis experiments. *Geochimica et Cosmochimica Acta*, 77, 275–291. <https://doi.org/10.1016/j.gca.2011.11.006>

Rout, R. K., & Tripathy, G. R. (2024). Net effect of chemical erosion in a tropical basin on carbon cycle: Constraints from elemental and sulfur isotopic composition of the Mahanadi river water. *Chemical Geology*, 644, 121859. <https://doi.org/10.1016/j.chemgeo.2023.121859>

Saintilan, N. J., Archer, C., Maden, C., Samankassou, E., Bernasconi, S. M., Szumigala, D., et al. (2023). Metal-rich organic matter and hot continental passive margin: Drivers for Devonian copper-cobalt-germanium mineralization in dolomitized reef-bearing carbonate platform. *Mineralium Deposita*, 58(1), 37–49. <https://doi.org/10.1007/s00126-022-01123-1>

Santos, I. R., Burnett, W. C., Misra, S., Suryaputra, I., Chanton, J. P., Dittmar, T., et al. (2011). Uranium and barium cycling in a salt wedge subterranean estuary: The influence of tidal pumping. *Chemical Geology*, 287(1–2), 114–123. <https://doi.org/10.1016/j.chemgeo.2011.06.005>

Schaller, T., Morford, J., Emerson, S. R., & Feely, R. A. (2000). Oxyanions in metalliferous sediments: Tracers for paleoseawater metal concentrations? *Geochimica et Cosmochimica Acta*, 64(13), 2243–2254. [https://doi.org/10.1016/S0016-7037\(99\)00443-3](https://doi.org/10.1016/S0016-7037(99)00443-3)

Schlesinger, W. H., Klein, E. M., & Vengosh, A. (2017). Global biogeochemical cycle of vanadium. *Proceedings of the National Academy of Sciences*, 114(52), E11092–E11100. <https://doi.org/10.1073/pnas.1715500114>

Schmidtko, S., Stramma, L., & Visbeck, M. (2017). Decline in global oceanic oxygen content during the past five decades. *Nature*, 542(7641), 335–339. <https://doi.org/10.1038/nature21399>

Schopka, H. H., & Derry, L. A. (2012). Chemical weathering fluxes from volcanic islands and the importance of groundwater: The Hawaiian example. *Earth and Planetary Science Letters*, 339, 67–78. <https://doi.org/10.1016/j.epsl.2012.05.028>

Scott, C., & Lyons, T. W. (2012). Contrasting molybdenum cycling and isotopic properties in euxinic versus non-euxinic sediments and sedimentary rocks: Refining the paleoproxies. *Chemical Geology*, 324, 19–27. <https://doi.org/10.1016/j.chemgeo.2012.05.012>

Selby, D., & Creaser, R. A. (2003). Re–Os geochronology of organic rich sediments: An evaluation of organic matter analysis methods. *Chemical Geology*, 200(3–4), 225–240. [https://doi.org/10.1016/s0009-2541\(03\)00199-2](https://doi.org/10.1016/s0009-2541(03)00199-2)

Selby, D., & Creaser, R. A. (2005). Direct radiometric dating of hydrocarbon deposits using rhenium–osmium isotopes. *Science*, 308(5726), 1293–1295. <https://doi.org/10.1126/science.1111081>

Selby, D., Creaser, R. A., & Fowler, M. G. (2007). Re–Os elemental and isotopic systematics in crude oils. *Geochimica et Cosmochimica Acta*, 71(2), 378–386. <https://doi.org/10.1016/j.gca.2006.09.005>

Sen, I. S., & Peucker-Ehrenbrink, B. (2012). Anthropogenic disturbance of element cycles at the Earth's surface. *Environmental Science & Technology*, 46(16), 8601–8609. <https://doi.org/10.1021/es301261x>

Severmann, S., & Anbar, A. D. (2009). Reconstructing paleoredox conditions through a multitracer approach: The key to the past is the present. *Elements*, 5(6), 359–364. <https://doi.org/10.2113/gselements.5.6.359>

Sheen, A. I., Kendall, B., Reinhard, C. T., Creaser, R. A., Lyons, T. W., Bekker, A., et al. (2018). A model for the oceanic mass balance of rhenium and implications for the extent of Proterozoic ocean anoxia. *Geochimica et Cosmochimica Acta*, 227, 75–95. <https://doi.org/10.1016/j.gca.2018.01.036>

Shen, J., Papanastassiou, D., & Wasserburg, G. (1996). Precise Re-Os determinations and systematics of iron meteorites. *Geochimica et Cosmochimica Acta*, 60(15), 2887–2900. [https://doi.org/10.1016/0016-7037\(96\)00120-2](https://doi.org/10.1016/0016-7037(96)00120-2)

Shirey, S. B., & Walker, R. J. (1998). The Re-Os isotope system in cosmochemistry and high-temperature geochemistry. *Annual Review of Earth and Planetary Sciences*, 26(1), 423–500. <https://doi.org/10.1146/annurev.earth.26.1.423>

Small, M., Germani, M. S., Small, A. M., Zoller, W. H., & Moyers, J. L. (1981). Airborne plume study of emissions from the processing of copper ores in southeastern Arizona. *Environmental Science & Technology*, 15(3), 293–299. <https://doi.org/10.1021/es00085a004>

Smoliar, M. I., Walker, R. J., & Morgan, J. W. (1996). Re-Os ages of group IIA, IIIA, IVA, and IVB iron meteorites. *Science*, 271(5252), 1099–1102. <https://doi.org/10.1126/science.271.5252.1099>

Sproson, A. D., Selby, D., Gannoun, A., Burton, K. W., Dellinger, M., & Lloyd, J. M. (2018). Tracing the impact of coastal water geochemistry on the Re-Os systematics of macroalgae: Insights from the basaltic terrain of Iceland. *Journal of Geophysical Research: Biogeosciences*, 123(9), 2791–2806. <https://doi.org/10.1029/2018jg004492>

Stumm, W., & Sulzberger, B. (1992). The cycling of iron in natural environments: Considerations based on laboratory studies of heterogeneous redox processes. *Geochimica et Cosmochimica Acta*, 56(8), 3233–3257. [https://doi.org/10.1016/0016-7037\(92\)90301-x](https://doi.org/10.1016/0016-7037(92)90301-x)

Sun, W., Bennett, V., Eggins, S., Arculus, R., & Perfit, M. (2003). Rhenium systematics in submarine MORB and back-arc basin glasses: Laser ablation ICP-MS results. *Chemical Geology*, 196(1–4), 259–281. [https://doi.org/10.1016/s0009-2541\(02\)00416-3](https://doi.org/10.1016/s0009-2541(02)00416-3)

Sundby, B., Martinez, P., & Gobbel, C. (2004). Comparative geochemistry of cadmium, rhenium, uranium, and molybdenum in continental margin sediments. *Geochimica et Cosmochimica Acta*, 68(11), 2485–2493. <https://doi.org/10.1016/j.gca.2003.08.011>

Survey, U. S. G. (2023). Mineral commodity summaries 2023. Retrieved from <https://pubs.usgs.gov/publication/mcs2023>

Suttle, A., Jr., & Libby, W. (1954). Natural radioactivity of rhenium. *Physical Review*, 95(3), 866–867. <https://doi.org/10.1103/physrev.95.866.2>

Syvitski, J. P., Kettner, A. J., Correggiari, A., & Nelson, B. W. (2005). Distributary channels and their impact on sediment dispersal. *Marine Geology*, 222, 75–94. <https://doi.org/10.1016/j.margeo.2005.06.030>

Tabasi, S., Hassani, H., & Azadmehr, A. (2018). Field study on Re and heavy metal phytoextraction and phytomining potentials by native plant species growing at Sarcheshmeh copper mine tailings, SE Iran. *Journal of Mining and Environment*, 9(1), 183–194.

Tagami, K., & Uchida, S. (2004). Comparison of transfer and distribution of technetium and rhenium in radish plants from nutrient solution. *Applied Radiation and Isotopes*, 61(6), 1203–1210. <https://doi.org/10.1016/j.apradiso.2004.05.074>

Tagami, K., & Uchida, S. (2008). Rhenium contents in Japanese river waters measured by isotope dilution ICP-MS and the relationship of Re with some chemical components. *Journal of Nuclear Science and Technology*, 45(sup6), 128–132. <https://doi.org/10.1080/00223131.2008.10875993>

Tank, S. E., McClelland, J. W., Spencer, R. G., Shiklomanov, A. I., Suslova, A., Moatar, F., et al. (2023). Recent trends in the chemistry of major northern rivers signal widespread Arctic change. *Nature Geoscience*, 16(9), 789–796. <https://doi.org/10.1038/s41561-023-01247-7>

Taran, Y. A., Hedenquist, J., Korzhinsky, M., Tkachenko, S., & Shmulovich, K. (1995). Geochemistry of magmatic gases from Kudravy volcano, Iturup, Kuril islands. *Geochimica et Cosmochimica Acta*, 59(9), 1749–1761. [https://doi.org/10.1016/0016-7037\(95\)00079-f](https://doi.org/10.1016/0016-7037(95)00079-f)

Taylor, S. R., & McLennan, S. M. (1985). *The continental crust: Its composition and evolution*. Blackwell Scientific.

Trenberth, K. E., Smith, L., Qian, T., Dai, A., & Fasullo, J. (2007). Estimates of the global water budget and its annual cycle using observational and model data. *Journal of Hydrometeorology*, 8(4), 758–769. <https://doi.org/10.1175/jhm600.1>

Tripathy, G. R., Hannah, J. L., Stein, H. J., Gebo, N. J., & Ruppert, L. F. (2015). Radiometric dating of marine-influenced coal using Re-Os geochronology. *Earth and Planetary Science Letters*, 432, 13–23. <https://doi.org/10.1016/j.epsl.2015.09.030>

Turekian, K. K., & Luck, J.-M. (1984). Estimation of continental $^{187}\text{Os}/^{186}\text{Os}$ values by using $^{187}\text{Os}/^{186}\text{Os}$ and $^{143}\text{Nd}/^{144}\text{Nd}$ ratios in marine manganese nodules. *Proceedings of the National Academy of Sciences*, 81(24), 8032–8034. <https://doi.org/10.1073/pnas.81.24.8032>

Tzvetkova, C., Novo, L. A., Atanasova-Vladimirova, S., & Vassilev, T. (2021). On the uptake of rhenium by plants: Accumulation and recovery from plant tissue. *Journal of Cleaner Production*, 328, 129534. <https://doi.org/10.1016/j.jclepro.2021.129534>

Uchida, S., & Tagami, K. (2008). Concentrations and distributions of 9 major ions and 54 elements in major Japanese river waters. In M. Taniguchi (Ed.), *Headwaters to the ocean* (pp. 637–640). Taylor & Francis Group.

Van Sande, J., Massart, C., Beauwens, R., Schoutens, A., Costagliola, S., Dumont, J. E., & Wolff, J. (2003). Anion selectivity by the sodium iodide symporter. *Endocrinology*, 144(1), 247–252. <https://doi.org/10.1210/en.2002-220744>

Von Damm, K., Edmond, J. M., Grant, B., Measures, C., Walden, B., & Weiss, R. (1985). Chemistry of submarine hydrothermal solutions at 21° N, East Pacific Rise. *Geochimica et Cosmochimica Acta*, 49(11), 2197–2220. [https://doi.org/10.1016/0016-7037\(85\)90222-4](https://doi.org/10.1016/0016-7037(85)90222-4)

Vorlicek, T. P., Chappaz, A., Groskreutz, L. M., Young, N., & Lyons, T. W. (2015). A new analytical approach to determining Mo and Re speciation in sulfidic waters. *Chemical Geology*, 403, 52–57. <https://doi.org/10.1016/j.chemgeo.2015.03.003>

Vorlicek, T. P., Helz, G. R., Chappaz, A., Vue, P., Vezina, A., & Hunter, W. (2018). Molybdenum burial mechanism in sulfidic sediments: Iron-sulfide pathway. *ACS Earth and Space Chemistry*, 2(6), 565–576. <https://doi.org/10.1021/acsearthspacechem.8b00016>

Wagner, M., Chappaz, A., & Lyons, T. W. (2017). Molybdenum speciation and burial pathway in weakly sulfidic environments: Insights from XAFS. *Geochimica et Cosmochimica Acta*, 206, 18–29. <https://doi.org/10.1016/j.gca.2017.02.018>

Wagner, M., Hendy, I. L., McKay, J. L., & Pedersen, T. F. (2013). Influence of biological productivity on silver and redox-sensitive trace metal accumulation in Southern Ocean surface sediments, Pacific sector. *Earth and Planetary Science Letters*, 380, 31–40. <https://doi.org/10.1016/j.epsl.2013.08.020>

Wakoff, B., & Nagy, K. L. (2004). Perrhenate uptake by iron and aluminum oxyhydroxides: An analogue for pertechnetate incorporation in Hanford waste tank sludges. *Environmental Science & Technology*, 38(6), 1765–1771. <https://doi.org/10.1021/es0348795>

Wan, J., Tokunaga, T. K., Williams, K. H., Dong, W., Brown, W., Henderson, A. N., et al. (2019). Predicting sedimentary bedrock subsurface weathering fronts and weathering rates. *Scientific Reports*, 9(1), 17198. <https://doi.org/10.1038/s41598-019-53205-2>

Wang, W., Dickson, A., Stow, M., Dellinger, M., Hilton, R., Savage, P., et al. (2024). Rhenium elemental and isotopic variations at magmatic temperatures. *Geochemical Perspectives Letters*, 28, 48–53. <https://doi.org/10.7185/geochemlet.2402>

Wang, Y., Li, S., Xu, P., Wang, H., Chen, Y., & Chen, J. (2024). Rapid and significant perturbations on the global geochemical cycle of rhenium by human activities – a case study in Yangtze River basin. *Applied Geochemistry*, 162, 105912. <https://doi.org/10.1016/j.apgeochem.2024.105912>

Wedepohl, K. H. (1995). The composition of the continental crust. *Geochimica et Cosmochimica Acta*, 59(7), 1217–1232. [https://doi.org/10.1016/0016-7037\(95\)00038-2](https://doi.org/10.1016/0016-7037(95)00038-2)

White, J., & Cameron, A. (1948). The natural abundance of isotopes of stable elements. *Physical Review*, 74(9), 991–1000. <https://doi.org/10.1103/physrev.74.991>

Wong, M. Y., Rathod, S. D., Marino, R., Li, L., Howarth, R. W., Alastuey, A., et al. (2021). Anthropogenic perturbations to the atmospheric molybdenum cycle. *Global Biogeochemical Cycles*, 35(2), e2020GB006787. <https://doi.org/10.1029/2020gb006787>

Wu, T., Wang, Z., Li, Q., Pan, G., Li, J., & Van Loon, L. R. (2016). Re (VII) diffusion in bentonite: Effect of organic compounds, pH and temperature. *Applied Clay Science*, 127, 10–16. <https://doi.org/10.1016/j.clay.2016.03.039>

Xiong, Y., & Wood, S. A. (1999). Experimental determination of the solubility of ReO_2 and the dominant oxidation state of rhenium in hydrothermal solutions. *Chemical Geology*, 158(3–4), 245–256. [https://doi.org/10.1016/s0009-2541\(99\)00050-9](https://doi.org/10.1016/s0009-2541(99)00050-9)

Xiong, Y., Xu, J., Shan, W., Lou, Z., Fang, D., Zang, S., & Han, G. (2013). A new approach for rhenium(VII) recovery by using modified brown algae *Laminaria japonica* adsorbent. *Bioresource Technology*, 127, 464–472. <https://doi.org/10.1016/j.biortech.2012.09.099>

Xue, S., & Li, Y. (2022). Pyrrhotite–silicate melt partitioning of rhenium and the deep rhenium cycle in subduction zones. *Geology*, 50(2), 232–237. <https://doi.org/10.1130/g49374.1>

Yamashita, Y., Takahashi, Y., Haba, H., Enomoto, S., & Shimizu, H. (2007). Comparison of reductive accumulation of Re and Os in seawater–sediment systems. *Geochimica et Cosmochimica Acta*, 71(14), 3458–3475. <https://doi.org/10.1016/j.gca.2007.05.003>

Yang, J. S. (1991). High rhenium enrichment in brown algae: A biological sink of rhenium in the sea? *Hydrobiologia*, 211(3), 165–170. <https://doi.org/10.1007/bf00008532>

Yin, Q. Z., Jagoutz, E., Verkhovskiy, A. B., & Wänke, H. (1993). ^{187}Os – ^{186}Os and ^{187}Os – ^{188}Os method of dating: An introduction. *Geochimica et Cosmochimica Acta*, 57(16), 4119–4128. [https://doi.org/10.1016/0016-7037\(93\)90358-4](https://doi.org/10.1016/0016-7037(93)90358-4)

Yudovskaya, M. A., Tessalina, S., Distler, V. V., Chaplygin, I. V., Chugaev, A. V., & Dikov, Y. P. (2008). Behavior of highly-siderophile elements during magma degassing: A case study at the Kudryavy volcano. *Chemical Geology*, 248(3–4), 318–341. <https://doi.org/10.1016/j.chemgeo.2007.12.008>

Zelenski, M. E., Fischer, T. P., De Moor, J. M., Marty, B., Zimmermann, L., Ayalew, D., et al. (2013). Trace elements in the gas emissions from the Erta Ale volcano, Afar, Ethiopia. *Chemical Geology*, 357, 95–116. <https://doi.org/10.1016/j.chemgeo.2013.08.022>

Zhang, Y., Wang, J., Qu, Y., Zhu, C., & Jin, Z. (2024). Mobility of rhenium and selenium during chemical weathering and their implication for petrogenic organic carbon oxidation. *Science China Earth Sciences*, 67(3), 740–750. <https://doi.org/10.1007/s11430-023-1244-5>

Zhu, Z., & Zheng, A. (2017). Determination of rhenium in seawater from the Jiulong river estuary and Taiwan Strait, China by automated flow injection inductively coupled plasma–mass spectrometry. *Analytical Letters*, 50(9), 1422–1434. <https://doi.org/10.1080/00032719.2016.1233244>

Znamensky, V., Korzhinsky, M., Steinberg, G., Trachenko, S., Yakushev, A., Laputina, I., et al. (2005). Rheniite, ReS_2 , the natural rhenium disulphide from fumaroles of Kudryavy volcano, Iturup island, Kurile islands. Paper presented at the Proceedings of the Russian Mineralogical Society.

Zondervan, J. R., Hilton, R. G., Dellinger, M., Clubb, F. J., Roylands, T., & Ogric, M. (2023). Rock organic carbon oxidation CO_2 release offsets silicate weathering sink. *Nature*, 623(7986), 329–333. <https://doi.org/10.1038/s41586-023-06581-9>